Valorisation of olive mill wastewater by phenolic compounds adsorption: Development and application of a procedure for adsorbent selection

(Article begins on next page)

25 April 2024

# Valorisation of olive mill wastewater by phenolic compounds adsorption: development and application of a procedure for adsorbent selection

Dario Frascari[a,*], Giorgia Rubertelli[a], Fatma Arous[b], Alessandro Ragini[a], Letizia Bresciani[c], Antonio Arzu[d], Davide Pinelli[a]

*[a] Department of Civil, Chemical, Environmental and Materials Engineering, University of Bologna, Via Terracini 28, 40131 Bologna, Italy*

*[b] Laboratoire Microorganismes et Biomolécules Actives, Faculté des Sciences de Tunis, Université de Tunis El Manar, LR03ES03, 2092, Tunis, Tunisia*

*[c] Laboratory of Phytochemicals in Physiology, Human Nutrition Unit, Department of Veterinary Science, University of Parma, via Volturno 39, 43125 Parma, Italy*

*[d] DOW Italia Divisione Commerciale S.r.l., Via Albani 65, 20148 Milano, Italy*

[*] Corresponding author at: DICAM, University of Bologna, Via Terracini 28, 40131 Bologna, Italy. *E-mail* address: dario.frascari@unibo.it (D. Frascari).

**ABSTRACT**

A procedure for the selection of the optimal adsorbent for phenolic compounds (PC) recovery from PC-rich wastes and wastewaters was innovatively proposed and applied to compare 4 neutral resins (Amberlite XAD16N, Optipore SD-2, Amberlite FPX66, Amberlite XAD761) and 1 ion-exchange resin (Amberlite IRA958 Cl) for PC recovery from a Tunisian olive mill wastewater (OMW). In the initial batch isotherm tests a neutral resin (XAD16N) performed best thanks to its high PC sorption capacity (81 $mg_{PC}/g_{dry\ resin}$) and PC content in the sorbed product (0.19 $g_{PC}/g_{volatile\ solids}$). Also ion-exchange resin IRA958, used in OH form in this work, resulted interesting thanks to its satisfactory performances and very low cost (8 €/L). These two pre-selected resins were further compared by means of continuous-flow adsorption/desorption tests conducted in a 1-m packed column. The results indicate that if a low (20 %) breakpoint is selected, XAD16N leads to a PC-richer sorbed product (0.14 $g_{PC}/g_{volatile\ solids}$) and a higher operating capacity (0.30) than IRA958. Conversely, if a very high (90 %) breakpoint is selected, the two resins produce similar desorbed products in terms of both PC content (0.19-0.21 $g_{PC}/g_{volatile\ solids}$) and antioxidant capacity (4.6-4.9 $g_{ascorbic\ acid\ equivalent}/g_{PC}$). Resin-specific dynamic desorption procedures led to very high PC desorption yields (87-95 %). The identification of the actual PCs present in the final desorbed product indicated for XAD16N a higher capacity to preserve the integrity of the PC mixture of the studied OMW. OMW microfiltration (0.2 μm pore-size) led to a 99.8 % suspended solid removal - thus protecting the packed column from potential clogging - with a very low PC loss.

**Keywords:** phenolic compounds; adsorption; ion exchange; resin selection; antioxidant activity; olive mill wastewater.

## 1. Introduction

The production of olive mill wastewater (OMW) is extremely large: 23-26·$10^6$ $m^3_{OMW}$/y are produced in Mediterranean, where 98 % of the world olive oil production is concentrated. OMW constitutes a relevant environmental concern: its high COD (20-200 g/L) and the presence of 0.1-18 g/L of phenolic compounds (PCs) causes bad smell and inhibition of seed germination and of the aerobic and anaerobic biodegradation processes potentially applicable to make OMW suitable for irrigation [1-5]. Therefore, although untreated OMWs have traditionally been used to irrigate the olive tree fields, several countries have recently forbidden this practice, thus imposing OMW treatment. The main components of OMW are PCs, sugars and organic acids, together with valuable amount of minerals, especially potassium [1]. Generally, OMW contains about 95 % of the PC content of the original olives, as a result of the high solubility of PCs in water [6]. The main PC classes found in OMW are phenolic acids, secoiridoids and flavonoids, among which hydroxytyrosol, oleuropein and verbascoside are the most abundant and the most studied compounds [7-9]. However, OMW PC composition varies both qualitatively and quantitatively according to the olive variety, climate conditions, cultivation practices, the olive storage time and the olive oil extraction process [10]. PCs present strong antioxidant, anti-inflammatory and antimicrobial properties, and several health effect have been attributed to the consumption of polyphenol-rich foods [1, 11-17]. In particular hydroxytyrosol is one of the most valuable and expensive PCs, with a high demand in the pharmaceutical, food and cosmetic fields.

Several processes have been proposed by researchers and wastewater companies for the treatment of OMW: evaporation, ultrafiltration, reverse osmosis, flocculation, chemical oxidation, anaerobic digestion, lagooning [5]. Even though several combinations of these technologies can lead to a complete OMW treatment, the costs of the resulting process are particularly high, as a result also of the small scale of olive mills and of the seasonality of OMW production [5]. In addition, these processes do not include a specific treatment step aimed at the recovery of the PC content of OMW. On the other hand, the inclusion in the OMW treatment train of a step leading to PC recovery could lead to a relevant decrease of the OMW treatment cost. Several processes can be applied to recover PCs from OMW: solvent extraction [1, 17-19], membrane separation [20, 21], adsorption [22-26] and cloud point extraction [27].

Adsorption was successfully applied for PC recovery from different wastewater types [28-33]. It has a relatively simple design, operation and scale up. A significant drawback of this recovery technology is that, in the presence of a complex matrix such as OMW, the PC content of the final product can be significantly reduced by the competitive adsorption exerted by other compounds, in particular carbohydrates and amino acids [34]. Two adsorption mechanisms can be applied for PC recovery: simple adsorption on neutral non-ionic resins and ion exchange on ionic resins. Both processes were successfully used in several fields [22, 35]. pH has a relevant impact on PC adsorption: low pHs favour the protonated PC form and thus adsorption on neutral resins, whereas higher pHs favour the anionic PC form, and therefore the ion exchange mechanism. High pHs promote the ion exchange of PCs that do not contain carboxyl functional groups. On the other hand, the ion exchange of PCs that contain carboxyl groups can be operated also at neutral pH values [34].

Although several works deal with PC adsorption and recovery, most studies are limited to the selection of a suitable resin by means of batch tests, thus neglecting key parameters such as the resin operating efficiency and the actual desorption rate attainable under continuous flow conditions [36, 37]. A limited number of studies integrated batch isotherm tests with dynamic continuous-flow tests [38, 39], whereas none of these proposed a rigorous procedure for the selection of the optimal sorbent. In addition, only a small minority of these studies used an actual OMW [40, 41], whereas the others used other natural sources or synthetic PC mixtures.

The main goal of this work was to develop and apply a procedure for the selection of the optimal adsorbent for PC recovery from PC-rich wastewaters and – after a solvent extraction step – solid wastes. The proposed procedure guides the user towards the identification a resin with a high selectivity for PCs, so as to maximize the PC content and antioxidant capacity of the final desorbed product. The procedure includes also the maximization of the resin operating capacity, a key parameter in the determination of the process capital and operational costs. To this purpose, the procedure includes both batch and continuous-flow adsorption and desorption tests, and a detailed characterization of the final desorbed product. The proposed resin selection approach was applied to an actual OMW, produced by a Tunisian olive mill. The PC recovery process developed in this work represents the first step of an OMW treatment process consisting in the combination of adsorption with anaerobic digestion, aimed at producing an irrigation-quality treated OMW.

The main novelties of this study are:

i) The development and application of a sorbent selection procedure for the selective recovery of high added value compounds such as PCs. Indeed, procedures have been previously developed for the selection of the optimal sorbent in specific fields, such as the separation of $CO_2$ or volatile organic compounds from air [42, 43] or the removal of heavy metals from groundwater or wastewater [44]. However, even though several studies compared the capacity of different sorbents to adsorb PCs, a rigorous procedure for sorbent selection for PC recovery from complex organic wastes has not been published, to the best of our knowledge.

ii) The inclusion in the sorbent selection procedure of a combination of batch and continuous flow adsorption/desorption tests, and the assessment of the final desorbed products in terms of total PC content, antioxidant activity and presence of compounds of high economic value. Indeed, in the majority of the studies on antioxidant adsorption the comparison of the performances of different sorbents was limited to batch isotherm tests, that often neglected the desorption step. Given the strong differences between the operational conditions of batch and continuous-flow tests, the performance parameters (such as adsorption and desorption yields or desorbed product composition) obtained in the two types of tests can result different. In addition, only continuous-flow tests allow the evaluation of the resin operating capacity, a key parameter for the evaluation of the capital and operational costs of the process.

iii)The application of a rotary microfiltration process as a pre-treatment step before PC adsorption, to avoid the gradual clogging of the adsorption column.


## 2. Materials and Methods

## 2.1 OMW, resins and chemicals

The tested OMW was produced by a 3-phase olive mill located in Mnihla, Tunisia. Its characterization is reported in section 3.1.

Five sorbent resins, kindly provided by DOW Chemicals Europe GmbH, Horgen, Switzerland, were tested in the present work: Amberlite XAD16N, Optipore SD-2, Amberlite FPX66, Amberlite XAD761, Amberlite IRA958 Cl. Of these resins, 3 (XAD16N, FPX 66, XAD 761) are purely neutral adsorbents, one (IRA958 Cl) is a strong ion exchange resin, whereas Optipore SD-2 is a neutral adsorbent with a minor ion exchange component. The main characteristics of the 5 resins are reported in Table S1 in the Supplementary Material. The industrial cost of these resins varies in the 18-31 €/L range for the 4 neutral adsorbents, whereas the selected ion exchange resin (IRA 958 Cl) is significantly cheaper (8 €/L; Table S1). XAD16N, FPX 66, XAD 761 and Optipore SD-2 were activated as follows: 1) double washing with de-ionized (DI) water to remove salts: each step consists of a 10-minute washing under agitation at 140 rpm and subsequent liquid removal through a Whatman Phenomenex system connected to a vacuum pump; 2) double resin soaking with 0.5 % of HCl 0.1 mol/L in ethanol: each step consists of a 30 minute washing under agitation at 140 rpm and subsequent solvent removal; 3) the resulting slurry was re-washed with DI water as described in 1). IRA958 Cl was pre-treated in different ways depending on the resin form to be tested in the different assays: to test the Cl form, the resin was just rinsed in DI water. To test the OH form, the resin was rinsed in DI water, fluxed with NaOH 1 mol/L and eventually fluxed in DI water. All reagents and standards were purchased from Sigma Aldrich (Milan, Italy). The COD Test Tubes were acquired from Aqualytic (Dortmund, Germany).

## 2.2. Analytical methods

*Total PCs* were analysed by means of an HPLC method based on the use of an Agilent Infinity 1260 HPLC, equipped with a quaternary pump, an autosampler, a thermostatted column compartment, a Jasco 875-UV Intelligent UV/vis diode-array detector and a Phenomenex Kinetex® 2.6 μm Biphenyl 100 Å column (50 x 2.1 mm). Two mobile phases were applied (solvent A: HPLC-grade water with 0.1 % orthophosphoric acid; solvent B: acetonitrile). The flow was set at 1.0 mL/min and the mobile phase gradient (0-4 minutes, 100 % phase A; 4-6 minutes, 70 % phase A and 30 % phase B; 6-15 minutes 70 % phase A and 30 % phase B) was designed to merge all the phenolic peaks into a single broad peak. The wavelength was set a 264 nm and gallic acid was used as external standard (50 mg/L). In order to allow the comparison between the results of this work and those of previous studies of PC adsorption from OMW, the total PC content of the several samples of raw and microfiltered OMW and of the final desorbed products was measured also according to the conventional colorimetric test developed by Folin and Ciocalteu [45], applied as described in detail by Frascari et al. [25]. All the PC concentrations and PC-related parameters reported in this study refer to the HPLC method, unless otherwise indicated.

*Single PCs:* The samples were diluted 1:10 with acidified water (0.1 % formic acid, v/v) and the identification of the single PCs was performed as previously reported by Bresciani et al. [46] applying some modifications. An Accela UHPLC 1250 equipped with a linear ion trap-mass spectrometer (LTQ XL, Thermo Fisher Scientific Inc., San Jose, CA, USA) fitted with a heated-electrospray ionization probe (H-ESI-II; Thermo Fisher Scientific Inc., San Jose, CA, USA) was used. Separation was carried out by means of a Restek C18 (100x2.1 mm) column, 3 μm particle size (Restek Corporation, Bellefonte, PA, U.S.). The injection volume was 5 μL, and the column temperature 40 °C. PCs were detected in negative ionization mode, with mobile phase pumped at a flow-rate of 0.3 mL/min, consisting of a mixture of acidified acetonitrile (0.1 % formic acid) (solvent A) and 0.1 % aqueous formic acid (solvent B). Following 0.5 min of 5 % solvent A in B, the proportion of A was increased linearly to 51 % over a period of 8.5 min. Solvent A was increased to 80 in 0.5 min, maintained for 2 min and then the start condition were re-established in 0.5 min and maintained for 5 min to re-equilibrate the column (total run: 17 min). The H-ESI-II interface was set to a capillary temperature of 275 °C and the source heater temperature was 200 °C. The sheath gas ($N_2$) flow rate was set at 40 (arbitrary units) and the auxiliary gas ($N_2$) flow rate at 5. During PC analysis, the source voltage was 4.5 kV, and the capillary

voltage and tube lens voltage were -42 V and -118 V, respectively. A preliminary analysis of the single PCs was carried out by applying a negative ionization using a full-scan, data-dependent mode, scanning from a mass to charge (m/z) of 100-1500 using a collision induced dissociation (CID) equal to 35 (arbitrary units) to obtain fragmentation. Finally, further specific analyses, fragmenting the parent ion, were carried out to identify the compounds revealed in the first step, by monitoring specific m/z transitions. PCs were identified based on available scientific data [7, 8, 47].

*Antioxidant capacity* was measured by 2,2'-azino-bis(3-ethylbenzothiazoline-6-sulphonic acid; ABTS) decolorization assay using a Shimazu UV-VIS spectrophotometer (UV-1601). The ABTS stock solution was prepared by dissolving the ABTS reagent to a final concentration of 7 mM using a $K_2S_2O_7$ 2.5 mM solution and allowing the mixture to stand in the dark at room temperature overnight before use. The same day of the test an ABTS working solution (ABTS WS) was prepared using the stock solution by dilution with de-ionized water to an absorbance of $0.70 \pm 0.02$ at 734 nm. 10-100 µL of sample were then added to 1 mL of the ABTS WS and incubated at 30 °C for 30 minutes in a dark environment, and the absorbance value was read at 734 nm. The calibration line was obtained using ascorbic acid as standard. To calculate the antioxidant activity of the sample as $\mu g_{ascorbic\ acid\ equivalent}/\mu L_{sample}$, the following expression was applied:

$$\text{Antioxidant Activity} \left( \mu g\ \text{ascorbic acid eq.} / \mu L\ \text{sample} \right) = \frac{\text{Value calulated from calibration line (µg ascorbic acid eq.)} \times \text{sample dilution factor}}{\text{Sample volume reacted with 1mL ABTS WS (µL sample)}}$$

*Total solids* were measured by drying the sample overnight at 105 °C and weighing. *Volatile solids* were measured by exposing the 105 °C-dried sample at 550 °C overnight and re-weighing. *Suspended solids* were determined by filtration with a 0.45 µm ALBET cellulose nitrate membrane filter and weighing. *Dissolved solids* were determined as the difference between total and suspended solids. COD was measured spectrophotometrically using the Aqualytic COD Vario Tubes (range: 0-1500 $mg_{O2}/L$).

*Proteins* were spectrophotometrically analyzed following the Bradford method [48] by mixing 67 µL of sample with 2 mL of Bradford reagent (VWR International S.r.l). After an incubation of 10 minutes at 4 °C in a dark environment, absorbance was read at 595 nm. The calibration line was obtained using Bovin Serum Albumin (BSA) as standard. *Reducing sugars* were spectrophotometrically analyzed following the dinitrosalicylic acid (DNS) assay [49] by mixing 100 µL of sample, 100 µL of demineralized water and 100 µL of DNS (2-hydroxy-3,5-dinitrobenzoic acid) reagent. The mixtures were heated in boiling water for 15 minutes, cooled in ice to ambient temperature and after the addition of 900 µL the absorbance value was read at 540 nm. The calibration line was obtained using glucose as standard. The DNS reagent was prepared mixing 20 mL of a 96 mM DNS water solution with 8 mL of a 5.3 M Sodium potassium tartrate tetrahydrate basic solution (NaOH 2 mol/L), bringing the solution to a final volume of 40 mL.

*OMW density* was measured by means of a 100 mL ITI Tooling pycnometer. *pH* was measured with an EUTECH Instruments pH 2700 Series pH-meter (Thermoscientific, Walthman, Massachusetts). More details on the analytical procedures are reported in [25]. In the frontal analysis tests aimed at studying the fluid dynamic behavior of the adsorption bed, *electrical conductivity* (EC) was measured at the column outlet with an EUTECH Instruments 2700 series conductimeter (Thermoscientific, Walthman, Massachusetts).

## 2.3. OMW microfiltration

OMW microfiltration resulted necessary to avoid the adsorption bed clogging. The microfiltration plant, supplied by Juclas srl (Verona, Italy), was composed by: a 50 L feed reservoir, a membrane pump with a 1-4 bar operating pressure, a ceramic circular filter (40 cm diameter, 0.2 µm average pore-size), a manual valve to regulate the flowrate of the recirculated retentate and the filtration pressure, a pressure sensor in the retentate line to monitor and control the process, and two outlet streams: one for the permeated filtered OMW and one for the retentate, recirculated into the feed reservoir. The plant applies a cross flow

filtration, in which the suspension passes tangentially along the surface of the filter. A picture and the flow-sheet of the microfiltration unit, as well as a more detailed description of the principle of operation, are reported in Fig. S1 in the Supplementary Material.

## 2.4. Phenolic compounds and COD adsorption and desorption isotherms

The PC and COD adsorption isotherms relative to the 5 tested resins were studied by mixing different amounts of dry resin with 30 mL of microfiltered OMW in 120 mL glass vials, so as to test dry resin / OMW ratios in the 2-450 $g_{dry\ resin}$/L range. The vials were placed in a rotatory shaker (120 rpm, 22 °C) for 2 hours, to reach the equilibrium condition. Preliminary tests aimed at selecting the optimal pH for the investigated resins performed at 10 $g_{dry\ resin}$/L$_{OMW}$. A graphical representation of the procedure for resin activation and for the operation of the batch adsorption tests is provided in Fig. S2 in the Supplementary Material.

The PC concentration in the liquid was evaluated by HPLC. For both PC and COD, the equilibrium concentration in the solid phase, $C_{S,i,eq}$ was determined as:

$$C_{S,,eq,i} = (C_{L,0,i} \cdot V_{OMW,0} - C_{L,eq,i} \cdot V_{L,final})/m_S \tag{1}$$

where: $m_S$ indicates the dry resin mass, $C_{L,0,i}$ and $C_{L,eq,i}$ the initial and final PC or COD concentrations in the liquid phase, $V_{OMW,0}$ and $V_{L,final}$ the OMW volume initially added and the final liquid volume resulting from the sum of the added OMW and the water initially contained in the activated resin. 95 % confidence intervals associated to $C_{S,eq,i}$ were calculated by means of standard error propagation rules.

In order to gain more insight on the type of adsorption mechanisms and to be sure that the equilibrium condition had been reached after the 2 hour equilibration time, a preliminary adsorption kinetic test was conducted for each tested resin at the higher resin concentration tested in the isotherm (450 $g_{dry\ resin}$/L). During these tests, the PC liquid-phase concentrations were frequently measured every for 180 minutes. The corresponding dimensionless sorbed-phase PC concentrations ($C^*_{S,t,PC} = C_{S,\ t,PC}\ /\ C_{S,eq,PC}$, where $C_{S,eq,PC}$ indicates the average sorbed-phase concentration during the last 30 minutes of each test) were plotted versus time and interpreted with both the first-order or Lagergren model ($dC^*_{S,t,PC}/dt = k_1 \cdot \left(C^*_{S,eq,PC} - C^*_{S,t,PC}\right)$) and the pseudo-second-order model ($dC^*_{S,t,PC}/dt = k_2 \cdot \left(C^*_{S,eq,PC} - C^*_{S,t,PC}\right)^2$) [50].

For each resin, the performance parameters obtained from the isotherms were the PC sorbed concentration ($C_{S,PC,eq,OMW}$) and the purity in PCs of the sorbed product (PC/volatile solids) in equilibrium with the PC and COD average concentration in the microfiltered OMW. Indeed, in a continuous flow adsorption process characterized by a high resin operating capacity, in most of the adsorbing bed the solid phase is in equilibrium with the PC and COD concentrations of the treated OMW. The correct evaluation of these parameters requires a model-based extrapolation of the isotherm experimental data until the PC and COD concentrations of the treated OMW ($C_{L,PC,OMW}$, $C_{L,COD,OMW}$), since all the experimental data at equilibrium are necessarily characterized by liquid phase PC and COD levels lower than the corresponding ones in the treated OMW. To this purpose, the PC and COD experimental isotherms were interpolated by means of the Langmuir (Eq. (2)) and Freundlich (Eq. (3)) models:

$$Langmuir \qquad C_{S,eq,i} = \frac{C^{\infty}_{S,i} \cdot C_{L,eq,i}}{\frac{1}{K_{eq,i}} + C_{L,eq,i}} \tag{2}$$

$$Freundlich \qquad C_{S,eq,i} = K_{F,i} \cdot C_{L,eq,i}^{1/n_i} \tag{3}$$

where: $C_{S,eq,i}$ ($g_i$/$g_{dry\ resin}$) and $C_{L,eq,i}$ ($g_i$/L) indicate respectively the amount of sorbed PCs or COD per unit mass of adsorbent and the PCs or COD concentration in the liquid phase at equilibrium; $C_{S,i}^{\infty}$ ($g_i$/$g_{dry\ resin}$) the maximum amount sorbed per unit mass of adsorbent, corresponding to a complete monolayer on the adsorbent surface; $K_{eq,i}$ (L/$g_i$) the constant related to the affinity between the binding sites and PCs or COD; $K_{F,i}$ (L/$g_{dry\ resin}$) the sorption capacity in the Freundlich model; $1/n_i$ (-) the sorption intensity in the Freundlich model. The simulation of the isotherm experimental data was limited to the Langmuir and Freundlich models as the vast majority of the studies on the application of adsorption to liquid streams limited the simulation activities to these two models and obtained very high correlation coefficients with either the

Langmuir or the Freundlich model [e.g., 41, 51, 52]. Furthermore, in this work the goal of the isotherm modeling activity was not to identify the most suitable model among the numerous ones available in the literature, but rather to perform a model-based evaluation of the two above-listed performance parameters, which requires the extrapolation of the PC and COD sorbed concentrations up to the values obtained in equilibrium with the corresponding levels in the treated OMW.

The model parameters were estimated by non-linear least squares regression of the calculated COD or PC solid phase concentrations ($C_{S,eq,calc,i}$) to the corresponding experimental values ($C_{S,eq,i}$). For each tested resin and parameter (PC or COD) the best-fitting model was selected on the basis of the correlation coefficient $R^2$, defined so as to take into account the number of model parameters [53]:

$$R^2 = 1 - \left( \frac{\sum_{i=1}^{N} \left( C_{S,eq,i} - C_{S,eq,calc,i} \right)^2}{N - P - 1} \right) \bigg/ \left( \frac{\sum_{i=1}^{N} \left( C_{S,eq,i} - C_{S,eq,m} \right)^2}{N - 1} \right)$$

where $N$ indicates the number of experimental tests in the studied isotherm, and $P$ the number of model parameters. For each isotherm, the Langmuir and Freundlich isotherms were compared by means of F tests. The best-fitting model was considered statistically different from the other one if the test outcome – indicating the probability that the two models are not statistically different - resulted $< 0.05$. The 95% confidence intervals (CI) associated to the best fitting parameters were determined according to the procedure illustrated by Smith et al. [54]. The 95% CI associated to the performance parameters estimated from the isotherm tests were estimated from the 95% CI of the best fitting model parameters, on the basis of standard error propagation rules.

For the resins that led to the best adsorption performances, the adsorption tests were followed by batch desorption tests. To this purpose, the OMW in equilibrium with the tested resin was removed by gravity filtration through a 100 µm mesh, and 30 mL of each tested desorption solvent (see section 3.3.3 for details) were added to the retained resin. The vials were placed again in a rotatory shaker (120 rpm, 22 °C) for 2 hours, to reach the equilibrium condition. Total PCs were then measured in the liquid phase. In some desorption tests, after the 2-hour contact time the resin was separated from the desorption solvent by filtration and re-used for further desorption steps, as illustrated in more detail in section 3.3.3. A graphical representation of the procedure for the operation of the batch desorption tests is provided in Fig. S3 in the Supplementary Material.

The desorption performances of each resin / solvent combination were quantified by means of the PC desorption yield ($Y_{des,PC,}$), evaluated as $m_{PC, desorbed} / m_{PC,sorbed}$. The results were utilized to select for each resin the best desorption solvent(s) and the corresponding optimal pH.

## 2.5. Adsorption column packing and fluid-dynamic characterization

The adsorption/desorption breakthrough tests, performed only for the resins that provided satisfactory performances in the batch isotherm tests, were conducted at 22 °C in a plant composed of 2 glass columns (height 0.61 m, inner diameter 0.027 m) connected in series. The flow-sheet and a picture of the plant are represented in Fig. 1. The column temperature was controlled at 22 °C by means of a jacket connected to a temperature-controlled bath. After placing a 55 mm layer of quartz sand at the bottom, each column was filled with the chosen resin using the dynamic axial compression technique described previously [25, 32]. Finally, a further 55 mm quartz sand layer was placed at the top of the resin. The total resin bed length was thus 1.00 m. For each resin tested in the semi-continuous assays, the fluid dynamic behavior of the adsorption bed was studied before each adsorption/desorption experiment by means of conventional frontal analysis tests conducted with a 0.05 mol/L NaCl solution in the case of neutral resins. In the case of the IE resin IRA958 OH, given the very high affinity of Cl⁻ for the resin functional group, a different approach based on the use of Cl⁻ free solutions was selected: a first test was conducted with a NaOH 0.05 mol/L solution, after fluxing the packed resin with de-ionized water, whereas a second test was conducted with de-ionized water, after fluxing the packed resin with NaOH 0.05 mol/L. These tests were used in the first place to estimate the effective porosity ($\varepsilon$), a parameter required to evaluate the interstitial

velocity and the hydraulic retention time on the basis of the measured OMW flow rate. The effective porosity was evaluated from the retention time distribution curve according to the procedure proposed by Levenspiel [55]. The frontal analysis tests were also used to evaluate two indicators of packing quality: the reduced plate height, evaluated as ratio of the height equivalent to a theoretical plate (HETP) to the mean particle diameter of the tested resin, and the asymmetry factor, defined as the ratio between the leading and tailing semi-width of the peak at 10 % of the peak height. These parameters were evaluated as described by Frascari et al. [25].

## 2.6. Adsorption/desorption breakthrough tests

The adsorption/desorption breakthrough tests, performed only for the resins that provided satisfactory performances in the batch isotherm tests, were conducted at 22 °C in the 1.00-m column. During the adsorption step, the microfiltered OMW was fed with a Masterflex L/S 0.1 HP 1-100 RPM peristaltic pump. Both pressure drop and flowrate were measured hourly. The total PC and COD concentrations were measured in OMW samples taken every hour from the column exit and every 3 hours from the inlet. The average PC and COD levels at the inlet were used to normalize the corresponding outlet values. The adsorption tests were continued up to the attainment of a 0.92-0.95 outlet normalized PC concentration. The adsorption performances of each tested resin were quantified by means of the following indicators, referred to a 0.20 PC dimensionless outlet concentration used as breakpoint value: i) PC and VS adsorption yield ($Y_{ads,i}$), evaluated as $m_{i,\ sorbed}\ /\ m_{i,fed}$; ii) resin selectivity for PCs, or PC/VS enrichment factor, defined as the PC/VS ratio of the adsorbed matter over that in the microfiltered OMW; the latter parameter corresponds to the ($Y_{ads,PC}/Y_{ads,VS}$) ratio; iii) resin operating capacity ($\eta_{resin}$), defined as (PC mass sorbed at the breakthrough point) / (total PC mass that could be sorbed if all the resin was saturated). The VS adsorption yield was evaluated on the basis of the COD values measured during each breakthrough test, given the impossibility to accurately measured VS in the 2 mL samples periodically taken during each test. The detailed procedure relative to the evaluation of these performance indicators is reported in Table S2 in the Supplementary Material. The 95% CI associated to the estimated performance parameters were calculated by means of standard error propagation rules.

Different desorption solvents and procedures were used for each resin, on the basis of the results of the batch desorption tests and of previous works [2, 25, 32, 56]. The desorption solvent was fed with a Masterflex L/S 0.1 HP -1-100 RPM pump in counter-current flow with respect to adsorption step. The solvent flowrate was initially equal to the OMW flow rate in the corresponding adsorption test. A regular decrease in solvent flowrate was then applied to maintain the total pressure at the column inlet < 2 bars, as solvent viscosity increased due to the increase in PC dissolved concentration. Desorption was stopped when a PC concentration < 1 % of the average inlet concentration during the adsorption step was attained.

The desorption performances of each tested resin were quantified by means of the PC and VS desorption yield ($Y_{des,i}$), evaluated as $m_{i,\ desorbed}\ /\ m_{i,sorbed}$; $m_{i,\ desorbed}$ and $m_{i,sorbed}$ were evaluated as illustrated in Table S2 in the Supplementary Material. In addition, the final desorbed product was characterized by means of the following parameters: i) specific antioxidant capacity; ii) purity in PCs, defined as PC/(volatile solids) and PC(total solids) mass fractions; iii) presence in the extract of high-value specific compounds, that could justify a further purification of the desorbed product.

# 3. Results and Discussion

## 3.1 Procedure for the identification of the most suitable resin(s), desorption solvent and operational conditions

The proposed procedure for the selection of a suitable resin and desorption solvent for the recovery of PCs from liquid agro-industrial wastes, and for the identification of the corresponding operational conditions, is articulated in the following 5 steps:

1. single point batch tests to identify the optimal pH for each resin
2. batch adsorption isotherms to evaluate the resin capacity for PCs and the sorbed product purity
3. batch desorption isotherms to select the desorption solvent for each resin
4. breakthrough adsorption tests to evaluate the resin selectivity for PCs and operating capacity
5. breakthrough desorption tests to evaluate the PC desorption yield and characterize the final product.

This procedure allows to estimate several performance parameters that can guide towards the selection of the most appropriate resin: resin capacity for PCs, purity in PCs of the sorbed and desorbed products, resin selectivity for PCs, resin operating capacity, PC adsorption / desorption yield, antioxidant capacity and composition of the final product. A schematic representation of the procedure is reported in Table S3 in the Supplementary Material, together with some additional details. A relevant drawback of the application of adsorption for the selective recovery of high added value compounds from complex mixtures is the fact that competitive adsorption exerted by other compounds could lead to a final product with a high concentration of undesired compounds [34]. For this reason, a relevant fraction of the above-listed performance parameters are aimed at quantifying the capacity of the resin to selectively adsorb PCs, thus leading to a final desorbed product with a high PC content and a high antioxidant capacity.

The first three steps of the procedure consist in batch test that can be conducted even at a very small scale (down to 2 mL), so as to minimize the amount of resin, liquid waste and desorption solvent required. Conversely, the last two steps consist in continuous flow breakthrough tests that typically require an adsorption column with a minimum 70-80 cm height and a large amount of liquid waste (to saturate the entire column) and desorption solvent. Therefore, the approach applied in this work to minimize the investigation cost and the amount of liquid waste required for the application of the proposed procedure, consists in using the small-scale batch tests (steps 1-3; section 3.3) for a pre-screening of the 2 most effective resins, which were further compared by means of breakthrough adsorption/desorption tests (steps 4-5; sections 3.4 and 3.5).

## 3.2. Characterization of the raw and microfiltered OMW

OMW microfiltration at 0.2 μm determined a 99.8 % suspended solids removal and a 9 % PC removal, associated to the PC content of the removed suspended particles. The average permeate flowrate was equal to 3 L/h, and each filtration process produced a final volume of concentrated sludge equal to 6 % of the treated OMW volume. On the basis of these results, the proposed microfiltration was considered an effective process for OMW pre-treatment before its adsorption in packed columns.

The main characteristics of the raw and microfiltered OMW are reported in Table 1. The studied OMW was characterized by a rather high COD (70 g/L). As shown in Table 2, 18 PCs were identified in the raw OMW: 9 phenolic acids and 9 phenylethanoids and secoiridoids, including compounds of high scientific and commercial interest [57,58], such as hydroxytyrosol, oleuropein and verbascoside.

## 3.3. Batch isotherm tests

The batch isotherm tests described in this section correspond to points 1-3 of the resin selection procedure illustrated in section 3.1 and Table S3.

### 3.3.1. Selection of the optimal form for resin IRA958 and of the optimal pH for the isotherm tests

Since the ion exchange resin IRA958 can be used both in Cl form (the form supplied by the resin provider) and in OH form, preliminary tests were aimed at selecting the optimal form to be used in this work. The affinity of Cl⁻ for a strong anion exchange resin (as IRA958) is 22 times higher than that of OH⁻ [59]. Therefore, the OH⁻/PC⁻ ion exchange is expected to be significantly more favorable than the Cl⁻/PC⁻ ion exchange. Preliminary batch tests confirmed that the PC sorption capacity of the OH form was significantly higher than that of the Cl form (data not shown). All the subsequent tests were therefore conducted with the OH form (indicated as IRA958 OH), attained by fluxing the resin with NaOH 1 mol/L.

The first step in the application of the resin selection procedure consists in the identification of the optimal pH for the tested resins. Indeed, PCs are a mixture of compounds exhibiting different acidic behaviors: some of them are carboxylic acids with an acid dissociation constant $K_a$ around $10^{-5}$, while others have a very low acidity due to the phenolic hydroxyl group ($K_a$ around $10^{-10}$). Therefore, at pH 5, about half of the carboxylic acids are dissociated and thus potentially sorbed on anionic IE resins. Conversely at pH 5 the phenols are almost completely protonated, and thus poorly sorbed on IE resins. At a pH = 13, 99.9 % of a phenolic compound with acidity similar to phenol is dissociated. At the same time, in case of IE resins, at very high pHs a strong competition is expected to be exerted by OH⁻ ions on the dissociated PCs. Conversely, for a neutral resin a better adsorption performance is expected when the PCs are not dissociated (neutral form), therefore at pH < 4-4.5.

For the 4 tested neutral resins (XAD16N, FPX 66, XAD 761 and Optipore SD-2), preliminary, single-point batch tests conducted in the 4.2-9.3 pH range indicated that, as expected, the equilibrium sorbed concentration decreases with increasing pH. As a representative example, the data relative to XAD16N are reported in Fig. 2. All the isotherms conducted with neutral resins were therefore operated at the OMW natural pH (equal to 4.2).

As for the IE resin (IRA958 OH), several batch adsorption tests were conducted in the 4.2-13 pH range. Starting from the natural pH of the filtered OMW (4.2), the desired pH values were attained by gradual additions of NaOH. Before adding the resin (10 g$_{dry\ resin}$/L$_{OMW}$), the samples were re-filtered at 0.2 μm, as some precipitate was observed at pH > 8. Furthermore, the antioxidant capacity of the pH-corrected OMW was measured at 6 pH values in the 4.2-13 range, in order to evaluate whether the possible changes in the OMW chemical composition had any effect on the antioxidant activity. As shown in Fig. S4 in the Supplementary Data, no significant effect of pH on the OMW antioxidant capacity was detected.

As illustrated in Fig. 2, the PC solid phase concentration increased in the 4.2-9 pH range thanks to the increased PC dissociation, whereas a small decrease was observed at pH > 9, possibly due to competition exerted by OH⁻. The subsequent tests relative to IRA958 were therefore conducted at pH 9. The increase in PC adsorption capacity observed with resin IRA958 OH in the 4.2-9 pH range is in agreement with the results of a previous study of PC recovery from OMW conducted with IRA958 Cl, XAD16N and IRA67 (a weak IE resin) [32]. Indeed, a pH increase from 4.9 to 7.2 determined a 20 % increase of the PC adsorption yield with IRA958 Cl, no relevant effect with the neutral resin XAD16N, and a 50 % decrease of the PC adsorption yield with the weak resin (IRA67), due to the shift of the resin functional group from the protonated active form to the unprotonated form.

### 3.3.2. Adsorption isotherms

The second step of the proposed resin selection procedure consists in the study of the PC and COD complete adsorption isotherms (T=22 °C) relative to the 5 tested sorbents at the previously selected pH values. The preliminary 3-hour kinetic adsorption tests, performed for each resin at the higher resin concentration tested in the isotherms (450 g$_{dry\ resin}$/L), indicated that the sorbed phase PC concentrations attained after 2 hour of shaking at 120 rpm were equal to 99-101 % of the final sorbed concentrations, calculated for each resin as the average of the sorbed-phase concentrations measured during the last 30 minutes of each 3-h test. On the basis of this result, the equilibration time was set to 2 hours for all the adsorption and desorption isotherm tests. The interpolation of the trends of dimensionless sorbed phase concentration versus time with both the first-order or Lagergren model and the pseudo-second-order model [50] resulted in $R^2$ values varying in the 0.94-0.99 range. For all the tested resins, the difference between

the $R^2$ values obtained with the two models did not result statistically significant (significance level = 0.05). As an example, the experimental data and the corresponding best-fitting simulations relative to resin XAD16N are shown in Fig. S5 in the Supplementary Material.

The results are shown in Fig. 3 in terms of solid and liquid phase equilibrium concentrations and best-fitting interpolation curves, whereas Table 3 reports the best-fitting parameters and the $R^2$ values obtained with both the Langmuir and Freundlich models for PCs, and only with the Freundlich model for COD. Indeed, all the COD isotherms present a strong upward curvature that excludes the possibility of successfully interpolating them with the Langmuir model. For each PC isotherm, the model (Langmuir or Freundlich) characterized by the highest $R^2$ was selected, and the statistical significance of the difference between the two interpolations was evaluated through an F test.

In the PC isotherms, the four non-ionic resins showed a favorable behavior (downward curvature) throughout the entire PC concentration range of interest (up to the PC concentration in the microfiltered OMW), whereas the PC isotherm of the IE resin IRA958 OH was basically linear. For resins XAD16N and FPX66 the Langmuir model resulted the best-fitting one, whereas for Optipore SD-2 the highest $R^2$ values were obtained with the Freundlich model. Conversely, for XAD761 and IRA958 OH the difference between the two models did not result statistically significant ($p > 5$ %). For these two resins, the model characterized by the highest $R^2$ was utilized for the subsequent data elaboration and displayed in Fig. 3. The quality of the best-fitting interpolations resulted very high for the 4 neutral resins ($R^2 = 0.98\text{-}0.99$), and high for IRA958 OH ($R^2 = 0.90$).

Overall, XAD16N resulted in the higher PC sorbed concentration almost over the entire tested concentration range (0.07-1.2 $g_{PC}$/L in the liquid phase), whereas Optipore SD-2 performed slightly better in the very low range ($< 0.07$ $g_{PC}$/L). A relevant resin performance parameter is $C_{S,PC,eqOMW}$, the sorbed PC concentration in equilibrium with the PC concentration in the microfiltered OMW, since it represents the sorbed concentration that will be achieved in most of the adsorbing bed in a continuous process characterized by a high operating capacity. Therefore, the higher $C_{S,PC,eqOMW}$, the lower the mass of resin needed to recover a given PC amount. $C_{S,PC,eqOMW}$ was calculated for each resin by extrapolating the selected isotherm up to the PC concentration in microfiltered OMW (1.28 $g_{PC}$/L). As shown in Table 3, with XAD16N $C_{S,PC,eqOMW}$ resulted equal to 81 $mg_{PC}$/$g_{dry\ resin}$, whereas for the other resins this parameter varied in the 47-67 $mg_{PC}$/$g_{dry\ resin}$ range. On the basis of the average conversion factor between Folin–Ciocalteu and HPLC method for the determination of total PCs obtained for the Tunisian OMW object of this work (2.6 $g_{PC\text{-}Folin}$ / $g_{PC\text{-}HPLC}$), the above-reported PC adsorption capacities correspond to 120-175 $mg_{PC\text{-}Folin}$/$g_{dry\ resin}$ if total PCs are expressed according to the Folin–Ciocalteu method. The significant difference obtained, for this specific OMW, between the PC content evaluated by HPLC and by Folin–Ciocalteu method can be ascribed primarily to the fact that both methods, when applied to the quantification of total PCs, apply one single response factor (that relative to gallic acid, by convention) to a wide list of compounds (Table 2) characterized by significantly different response factors. Therefore, both methods provide an indicator, but not an exact quantification, of the total PC concentration. In addition, Folin-Ciocalteu method has been reported to be responsive to other antioxidant molecules [60], being the reagent nonspecific to phenolic compounds [61, 62], since it can be reduced by nonphenolic compounds [63], thus leading to a possible overestimation of the estimated total PC concentration.

In order to compare the PC adsorption capacities obtained in this work with the corresponding ones reported in other studies of PC adsorption from OMW conducted with different types of sorbents, the sorbed-phase PC concentrations obtained in other studies in correspondence with the same PC concentration of the microfiltered OMW object of this study (4.0 $g_{PC\text{-}Folin}$/L) were evaluated on the basis of the best-fitting adsorption isotherms reported in each study examined. This analysis led to the evaluation of a PC sorption capacity of 40-160 $mg_{PC\text{-}Folin}$/$g_{dry\ resin}$ in batch tests conducted with resins XAD16N, XAD7, ENV+ and IRA96 [2], 190 $mg_{PC\text{-}Folin}$/$g_{dry\ resin}$ in batch tests conducted with activated carbon [64] and 450 $mg_{PC\text{-}Folin}$/$g_{dry\ resin}$ in batch tests conducted with peach-stone-derived activated carbon [41]. The PC sorption capacities obtained with the 5 resins tested in this work (120-175 $mg_{PC\text{-}Folin}$/$g_{dry\ resin}$) are therefore comparable to those reported in studies of PC recovery from OMW that focused on other adsorbent types.

Another relevant performance parameter that can be obtained by combining the PC and COD isotherms is the PC purity, or PC mass fraction, of the sorbed product. Indeed, a higher PC mass fraction

determines a higher specific antioxidant capacity, and therefore a higher market value of the desorbed product. This parameter, expressed as $g_{PC}/g_{COD}$, was calculated as the ratio (indicated as $C_{S,PC,eqOMW}$ / $C_{S,COD,eqOMW}$) of the PC to COD sorbed concentrations evaluated – by extrapolation of the best fitting isotherm for each resin – in correspondence of the PC or COD concentration in the microfiltered OMW used for the isotherms. This ratio corresponds to the purity of the sorbed product obtained, in a continuous-flow process, in the column fraction in equilibrium with both the PC and COD concentrations in the microfiltered OMW fed to the adsorption process. The product purity was then converted to $g_{PC}/g_{VS}$, by applying an average COD-VS conversion factor (2.9 $g_{O2}/g_{VS}$) obtained, in the second part of the work, by measuring COD and VS in different desorbed products. Volatile solids were not directly measured after each batch isotherm test, as such measurement requires a higher amount of OMW and resin than those used in these tests. As shown in Table 3, XAD16N and XAD761 resulted in the highest estimated PC purities (0.19-0.20 $g_{PC}/g_{VS}$), whereas for FPX66, OPTIPORE SD-2 and IRA958 OH the purities varied in the 0.07-0.12 $g_{PC}/g_{VS}$ range. It should be noted that these values, obtained from the batch isotherm tests, refer to the estimated PC content of the *sorbed* product, whereas the experimental measurement of the PC content of the *desorbed* product – the true final product of the process - was performed only for the breakthrough adsorption / desorption tests object of the second part of the work.

The overall evaluation of the isotherm tests led to the identification of XAD16N as the best-performing resin for PC recovery from the tested OMW, thanks to its highest PC sorption capacity and second-highest PC purity of the sorbed product. On the other hand, also IRA958 OH appeared to be an interesting resin, thanks to its very low cost (4 times lower than that of XAD16N) and to the attainment of (i) a PC sorption capacity in equilibrium with the OMW PC concentration equal to 80 % of that obtained with XAD16N, and (ii) a sorbed product PC purity equal to 2/3 of that obtained with XAD16N. Therefore, in the last part of the study XAD16N and IRA958 OH were further compared by means of continuous flow breakthrough tests of PC adsorption and desorption, corresponding to points 4 and 5 of the resin selection procedure illustrated in section 3.1 and Table S3.

### 3.3.3. Desorption isotherms

Before proceeding with the breakthrough tests, resins XAD16N and IRA958 OH were further investigated by means of batch desorption tests, aimed at performing a preliminary identification of the optimal desorption solvents and pH. These tests correspond to step 3 of the proposed resin selection procedure (section 3.1). In previous tests of desorption of OMW-derived PCs from resin XAD16N, ethanol acidified with 0.5 % v/v HCl 0.1 mol/L (pH 3.3) had been identified as the optimal desorption solvent [2, 25, 65]. Thus, in this work the first batch desorption tests for XAD16N were operated with pH 3.3 acidified ethanol. The results indicate that, while 1-step desorption led to quite low PC desorption yields (0.40-0.50), the operation of 5 consecutive batch desorptions with this solvent led to an overall PC desorption yield in the 0.50-0.65 range. In further attempts to increase the PC desorption yield from XAD16N, the best results were attained by operating – after 5 consecutive desorptions with acidified ethanol – 5 further desorption steps with a 50 % v/v mixture of de-ionized water and ethanol, acidified to pH 3.3 with HCl. This approach led for XAD16N to an overall PC desorption yield in the 0.75-0.80 range.

In order to desorb ionic compounds from an anionic IE resin, an anion characterized by a strong affinity for the tested resin must be supplied. The total moles of the selected desorption anion must be at least equal to the total moles of anions sorbed to the resin. As some physical adsorption can occur on the matrix of IE resins in addition to the actual IE process, the best desorption results are expected to be achieved if the selected anion is dissolved in a solvent effective in the desorption of physically-sorbed compounds. In this work, $OH^-$ and $Cl^-$ were compared as desorption anions for the adsorption tests conducted with IRA958 OH. In particular 4 types of desorption solutions were tested: NaOH in ethanol; NaCl in ethanol; HCl in ethanol; HCl in a 50 % v/v mixture of de-ionized water and ethanol. The best PC desorption yields (0.70 – 0.80) were obtained after 5 consecutive desorption steps conducted with a 50 % v/v mixture of de-ionized water and ethanol, acidified with HCl to a final concentration of 2 mol/L (pH - 0.3).

*3.4        Phenolic compounds and COD adsorption breakthrough tests*

The goal of the breakthrough tests performed with resins XAD16N and IRA958 OH (step 4 of the proposed procedure) was to evaluate crucial performance parameters that cannot be reliably estimated from the batch isotherm tests: the resin operating capacity for PCs ($\eta_{PC}$) and the PC and VS (or COD) adsorption yields ($Y_{ads,PC}$ and $Y_{ads,VS}$). Furthermore, the $Y_{ads,PC}$ / $Y_{ads,VS}$ ratio represents an indicator of the resin selectivity for PC, another key parameter in the resin selection process.

*3.4.1. Fluid-dynamic analysis of the column packings*

As a preliminary step, a fluid-dynamic analysis of the column packings made with both resins was performed. For XAD16N, the effective porosity resulted equal to 69.8 %, and the packing quality was rather good. Indeed, the asymmetry factor of the retention time distribution curve was very close to 1 (0.98) and the reduced plate height (47), even if quite high, fell in the range typical of columns packed with adsorption resins. As for the column packing made with IRA958 OH, in both type of tests performed with NaOH solutions (see section 2.5 for details) the retention time distribution curve resulted less symmetric (asymmetry factor in the 1.2-1.7 range). The effective porosity estimated from 4 tests conducted according to the two test types illustrated in section 2.5 resulted in an average value equal to 49.0 %. The reduced plate height (40-50) resulted similar to that obtained with XAD16N.

*3.4.2. Adsorption breakthrough tests*

One adsorption breakthrough test, fed with micro-filtered OMW, was performed for each tested resin (XAD16N and IRA958 OH). The operational conditions relative to these tests, reported in the upper part of Table 4, were selected on the basis of the following criteria:

- For resin XAD16N, in previous works of PC recovery from OMW [25, 32] the increase in resin bed height from 0.5 to 1.8 m and in *HRT* from 0.30 to 0.52 h, with a corresponding decrease in bed volumes / h (BV/h) from 2.8 to 1.7 BV/h, determined a 3.6-fold increase in resin operating capacity. In this work, in the attempt to find an intermediate solution characterized by design values close to the ones recommended in the resin datasheet (resin bed height > 0.75 m, BV/h > 2), the resin bed height was set to 1 m and the *HRT* to 0.30 h; consequently, considering the 0.70 packed resin porosity, the BV/h (equal to $\varepsilon$ / *HRT*) resulted equal to 2.3.

- For IRA958 OH, in the same previous works of PC recovery [25, 32], in tests conducted with a constant resin bed height of 1.8 m, the increase in *HRT* from 0.34 to 0.76 h, with a corresponding decrease in BV/h from 1.6 to 0.7, determined a 3.3-fold increase in resin operating capacity. In this work, the resin bed height and *HRT* were set to roughly the same values selected for resin XAD16N; consequently, considering the 0.49 packed resin porosity, the BV/h resulted equal to 1.47. These design values comply with the ones recommended in the resin datasheet in terms of bed height (> 0.60 m) but not in terms of BV/h (> 8), as previous studies showed that, in the specific case of PC adsorption from OMW, the high values of BV/h typically recommended for ion exchange resins lead to very low operating capacities [32]. The reason for this outcome could be that a physical adsorption of PCs on the resin acrylic matrix is likely to occur in parallel to the PC ion exchange on the resin functional group (quaternary ammonium).

The normalized PC and COD concentrations obtained at the column outlet during the two breakthrough tests are plotted with full symbols in Figs. 4a (XAD16N) and 4b (IRA958 OH) versus dimensionless time, defined as (actual time) / *HRT* in the resin bed. The tests were continued until the attainment of an outlet PC concentration equal to 87-91 % of the inlet concentration. The PC and COD experimental points were connected by interpolating lines drawn to make Fig. 4 more readable; these lines do not represent any process simulation. The same Figures includes for comparison purposes the PC and COD time plots obtained – under similar experimental conditions - in previous studies conducted with another OMW, significantly different than the Tunisian one object of this work. The results of this comparison will be discussed in the last part of this section.

The observation of Fig. 4 indicates in the first place that XAD16N, thanks to its high PC adsorption capacity and favourable isotherm, led to a rather slow PC release, with the 20 % PC breakpoint attained

after 13 HRTs. Conversely IRA958 OH, due to its lower PC adsorption capacity, features a more rapid PC release, with the 20 % breakpoint after just 4 HRTs. Also for COD the breakthrough obtained with XAD16N is less rapid than that obtained with IRA958 OH, even if in this case the difference is less marked.

The main performance parameters relative to these tests are reported in the lower part of Table 4. The PC adsorption yields evaluated at the 20 % breakthrough point were similar and very high (0.93-0.96), whereas IRA958 OH resulted in a significantly higher COD or VS adsorption yield than XAD16N (Table 4). As a result, for XAD16N the $Y_{ads,PC}$ / $Y_{ads,VS}$ ratio, that represents an indicator of resin selectivity for PCs, resulted quite high (3.6), in agreement with the favourable PC isotherm and unfavourable COD isotherm. Conversely, for IRA 958 OH the $Y_{ads,PC}$ / $Y_{ads,VS}$ ratio resulted 2.5 times lower.

For XAD16N, the PC operating capacity at the 20 % breakpoint resulted 3 times higher than that relative to IRA958 OH (Table 4). A low operating capacity plays unfavourably in the determination of the cost for the initial resin purchase and periodic resin replacement. The low operating capacity evaluated for IRA958 OH (about 0.10) suggests that this resin, as a result of its wide mass transfer zone, requires a higher bed length – and therefore a higher *HRT* - in order to operate under optimal conditions.

The elaboration of the PC and COD breakthrough curves allows to estimate the PC purity (or PC mass fraction) in the *sorbed* product at any point of the curve of normalized PC outlet concentration. Indeed, by dividing the PC and COD sorbed masses at any point of the curve by the mass of dry resin in the column experimentally measured during the packing procedure, one obtains the corresponding PC and COD sorbed concentration ($C_{S,PC}$ and $C_{S,COD}$). The detailed procedure for this calculation is reported in Table S2 in the Supplementary Material. The $C_{S,PC}$ / $C_{S,COD}$ ratio, an indicator of purity of the sorbed product, can then be converted to a $C_{S,PC}$ / $C_{S,VS}$ ratio by applying the average COD-VS conversion factor obtained by measuring COD and VS in different desorbed products (2.9 $g_{O2}/g_{VS}$). The sorbed product purity at the selected 20 % breakpoint resulted equal to 0.14 $g_{PC}/g_{VS}$ for XAD16N and 0.03 $g_{PC}/g_{VS}$ for IRA958 OH. For both resins, the sorbed product purity increased with time. At the end of the breakthrough test (a condition close to resin saturation) the estimated purities resulted significantly higher (0.22-0.39 $g_{PC}/g_{VS}$;  Table 4). The choice of the actual breakthrough point at which the adsorption process should be stopped depends on the goal of the process: if the technology is aimed at removing PCs from OMW for environmental reasons, the maximum PC concentration in the column outlet is set by a regulatory standard or law; conversely, if the goal is to produce a product characterized by a high PC content and therefore a high antioxidant capacity, no matter how much PC mass is released with the effluent, then a high breakpoint is likely to be the best option.

The breakthrough tests conducted with both resins were characterized by a roughly constant pressure drop equal to 0.2 bar for XAD16N and 0.30-0.35 bar for IRA058 OH. This result indicates that the 99.8 % suspended solid removal attained by the OMW microfiltration with a 0.2 μm average pore-size was effective in protecting the packed columns from potential clogging.

### 3.4.3. Adsorption performances obtained with a different OMW

For comparison purposes, Figs. 4a and 4b also show with empty symbols the PC and COD time plots obtained by the same research group, with the same two resins and with very similar HRTs (0.36-037 h), in previous tests conducted with an Italian OMW characterized, with respect to the Tunisian one object of this work, by a significantly lower COD (31 versus 70 g/L) and PC (0.6 versus 1.4 $g_{GA}/L$) concentration. The observation of Figs. 4a and 4b indicates that, for both resins, the use of a significantly different OMW led to very similar breakthrough dimensionless curves for both PCs and COD. More precisely, the OMW change determined a 3-5 % variation in PC adsorption yield and a 3-14 % variation in column operating efficiency (values estimated at a 20 % PC breakthrough). This important result indicates that the approach, methodology and main conclusions of this work can be applied also to OMWs with different characteristics.

### 3.5      Desorption / regeneration tests and desorbed product characterization

On the basis of the results of the batch desorption tests illustrated in section 3.3, the breakthrough test performed with resin XAD16N was followed by the application of a 2-step desorption procedure: the initial supply of 5 bed volumes of ethanol acidified with 0.5 % v/v HCl 0.1 mol/L (pH 3.3) was followed by 10 further bed volumes of a 50 % v/v mixture of de-ionized water and pH 3.3 acidified ethanol.

Conversely, the breakthrough test conducted with IRA958 OH was desorbed by supplying 7 bed volumes of a 50 % v/v mixture of de-ionized water and ethanol, acidified with HCl to a final concentration of 2 mol/L (pH -0.3).

These procedures led to the attainment of very high PC desorption yields (87-95 %) and to nearly complete VS desorption yields (Table 4). The characterization of the two desorbed products is reported in Table 5, whereas the list of the specific PCs identified in the two products is reported in the last two columns of Table 2. Coherently with the very high desorption yields, the final product purity attained with IRA958 OH ($0.19$ $g_{PC}/g_{VS}$) resulted very close to that estimated for the sorbed product ($0.22$ $g_{PC}/g_{VS}$; Table 4) whereas for XAD16N the final product purity ($0.21$ $g_{PC}/g_{VS}$) resulted equal to 55 % of the corresponding value estimated for the sorbed product. The product purity evaluated in terms of PC/total solids ratio ($0.18$-$0.20$ $g_{PC}/g_{TS}$) is 5-6 times higher than the corresponding value measured in the microfiltered OMW fed to the process, indicating that both the selected resins have a high selectivity for PCs. In addition, the measurement of the product purity based on the Folin–Ciocalteu method for PCs leads to estimate a significantly higher PC content in the desorbed product ($0.34$-$0.41$ $g_{PC\text{-}Folin}/g_{VS}$).

As shown in Table 2, the desorbed product obtained with XAD16N presented a complex variety of 28 PCs: 13 phenolic acids, principally represented by hydroxycinnamic and benzoic acid derivatives, 12 phenylethanoids and secoiridoids, as tyrosol, elanolic acid, verbascoside and oleuropein, 2 flavonoids and 1 lignan. With the exception of hydroxyelanolic acid, all the PCs detected in the raw OMW were identified also in the XAD16N product. Conversely, 11 PCs detected in the XAD16N extract were not found in the raw OMW, most likely because their initial concentration was below the method's detection limit. These findings confirm the high affinity of XAD16N for PCs. The desorbed product obtained with IRA958 OH presented a mixture of 20 PCs, including 9 phenolic acids and 11 phenylethanoids and secoiridoids. The adsorption/desorption process conducted with IRA958 OH led to the loss of 4 PCs initially detected in the raw OMW, whereas 8 PCs detected in the IRA958 OH extract were not found in the raw OMW due to their low initial concentration.

The detected PCs are generally recognized as potent antioxidants [66], antibacterials (gram positive and gram negative) and antifungals. They also demonstrated activities against yeast [67]. Their industrial application for these properties are increasing, both in the food industry, as reported for hydroxytyrosol and verbascoside in meat preparation [66, 68], or olive leaf phenolics in dairy preparation [69] and OMW extract for olive oil preservation [67], as well as in the cosmetic industries, as reported for oleuropein used as antiaging ingredient in cosmetic formulations [70].

Notwithstanding the modest differences in composition of the final PC mixture, the specific antioxidant activities of the products obtained with the two resins resulted quite close ($4.6$-$4.9$ $g_{AAeq}/g_{PC}$; Table 5), in agreement with the similar PC purities ($0.19$ $g_{PC}/g_{VS}$). The specific antioxidant activities of the two final products resulted comparable to that of the microfiltered OMW fed to the process ($5.3$ $g_{AAeq}/g_{PC}$). This finding indicates that the proposed adsorption/desorption process led to a satisfactory extraction and enrichment in PCs of the treated OMW, while maintaining roughly the same specific antioxidant activity. In order to assess the antioxidant capacity of the final products of this work, the same parameter was measured in single-compound solutions of two PCs well known for their high antioxidant activity and detected in both desorbed products, namely caffeic acid and hydroxytyrosol. The result obtained for the former ($1.7$ $g_{AAeq}/g_{PC}$) was lower than the values attained for the final desorbed products, whereas the antioxidant activity of hydroxytyrosol resulted about 2 times higher ($9.1$ $g_{AAeq}/g_{PC}$). This analysis indicates that both XAD16 and IRA958 OH led to the production of a PC-rich product characterized by a relatively high antioxidant activity.

## 4.    Conclusions

The proposed procedure provides a rigorous framework for the testing and selection of resins for PC recovery from PC-rich wastewaters and – after a solvent extraction step – solid wastes. The application of the procedure to a process of PC recovery from OMW confirmed that batch isotherm tests – typically used in the literature to compare resins for adsorption processes – need to be integrated by continuous-flow

adsorption / desorption tests. Indeed the latter allow to take into consideration several aspects and parameters not assessable by means of batch tests, such as the resin operating capacity and the effect of the selected breakpoint on the quality of the desorbed product.

The proposed resin selection procedure was successful in the identification of two resins (Amberlite XAD16N and Amberlite IRA958 OH) capable to produce a final mixture characterized by a high PC content and antioxidant capacity. The procedure thus contributes to the overcoming of a potential drawback of the application of adsorption to the recovery of high added value molecules from complex matrices, i.e. the risk that competitive adsorption leads to a relevant presence of undesired compounds in the final product. In particular, the batch isotherm tests allowed to make a preliminary identification of XAD16N and IRA958 OH as the most promising resins for PC recovery from the targeted Tunisian OMW. The subsequent continuous flow tests – limited to XAD16N and IRA958 OH – indicated that the final resin selection depends on the desired breakpoint, and therefore on the goal of the process. Indeed, if an environmental standard imposes in the column outlet a relatively low PC concentration, and therefore a low breakpoint, XAD16N led to a PC-richer product and a higher operating capacity than IRA958 OH, thanks to its higher PC selectivity and sorption capacity. Conversely, if the goal of the process is to produce a pure product characterized by a high PC purity and antioxidant capacity, no matter how much PC mass is released with the effluent, it is advisable to continue the adsorption step until the attainment of a very high breakpoint. In this case, the quality of the final products obtained with the two resins is similar, and IRA958 OH appears to be the most promising one thanks to its significantly lower industrial cost, despite its lower PC sorption capacity.

The identification of the actual PCs present in the final desorbed product – an aspect generally neglected in the literature – represents a useful integration of the product assessment in terms of antioxidant capacity and total PC content.

Lastly, OMW microfiltration with a 0.2 μm average pore-size proved to be an effective technology to attain a very high suspended solid removal - thus protecting the packed column from potential clogging - with a very low PC loss.

**List of abbreviations**

| | |
|---|---|
| V/h | ed Volumes / h |
| I | onfidence interval |
| OD | hemical oxygen demand |
| RT | ydraulic residence time |
| ɔ | n exchange |
| MW | live mill wastewater |
| ⊃ | ɔenolic compound |
| S | ɔtal solids |
| S | ɔlatile solids |

**Nomenclature**

| | |
|---|---|
| ₛ | symmetry factor, defined as ratio between the leading and tailing semi-width of the peak at 10 % of the peak height (-) |
| $_{L,i}$ | iquid phase concentration of compound $i$ ($g_{PC \text{ or } COD}$/L) |

| | |
|---|---|
| $_{L,0,i}$ , $C_{L,eq,i}$ | itial and final (equilibrium) PC or COD concentration in the liquid phase (OMW uring the isotherm tests ($g_{PC\ or\ COD}$/L) |
| $_{S,eq,calc,i}$ | OD or PC solid phase concentration calculated according to the Langmuir reundlich model, for the evaluation of the $R^2$ value associated to each isother $_{PC\ or\ COD}$/$g_{dry\ resin}$) |
| $_{S,eq,i}$ | nal (equilibrium) PC or COD concentration in the solid phase (resin) during tl otherm tests ($g_{PC\ or\ COD}$/$g_{dry\ resin}$) |
| $_{S,eq,m}$ | verage experimental solid phase concentration of compound $i$ in an isotherm tes or the evaluation of the $R^2$ value associated to each isotherm ($g_{PC\ or\ COD}$/$g_{dry\ resin}$) |
| $C_{S,eq,PC}^{*}$ | imensionless sorbed-phase PC concentration measured at equilibrium at the er the kinetic adsorption batch tests, calculated for each resin as the average of tl orbed-phase concentrations measured during the last 30 minutes of each 3-h te ) |
| $_{S,i}$ | olid phase (resin) concentration of compound $i$ ($g_{PC\ or\ COD}$/$g_{dry\ resin}$) |
| $_{S,i}^{\infty}$ | aximum amount sorbed per unit mass of adsorbent, in the Langmuir model (g $_{COD}$/$g_{dry\ resin}$) |
| $_{S,i,eqOMW}$ | C or COD solid phase (resin) concentration in equilibrium with the microfiltere MW used for the batch and breakthrough tests ($g_{PC}$/$g_{dry\ resin}$) |
| $C_{S,t,PC}^{*}$ | imensionless sorbed-phase PC concentration measured at time $t$ during the kinet lsorption batch tests (-) |
| $ETP$ | eight equivalent to a theoretical plate, in the packed column (m) |
| $_{eq,i}$ | onstant related to the affinity between the binding sites and PCs or COD, in tl angmuir isotherm ($L_{pore\ volume}$ /$g_{PC\ or\ COD}$) |
| $_{F,i}$ | e sorption capacity in the Freundlich model (L/$g_{dry\ resin}$) |
| $_{i,fed}$ | lass of PC or VS fed to the column until a certain breakpoint (mg) |
| $_{i,desorbed}$ | otal mass of PC or VS desorbed by the resin during the entire desorptic rocedure (mg) |
| $_{i,sorbed}$ | lass of PC or VS adsorbed by the resin in correspondence of a certain breakpoi 1g) |
| $_S$ | lass of dry resin in the isotherm studies ($g_{dry\ resin}$) |
| | iverse of the sorption intensity in the Freundlich model (-) |
| | umber of experimental points in each isotherm (-) |
| | umber of parameters to be estimated in each isotherm (-) |
| $_{OMW,0}$, $V_{L,final}$ | MW volume initially added and final liquid volume resulting from the sum of tl lded OMW and the water initially contained in the activated resin, in the isother sts (L) |
| $_{ds,i}$ | C or VS adsorption yield, calculated as $m_{PC\ or\ VS,sorbed}$ / $m_{PC\ or\ VS,initial}$ in the bat sts, and as $m_{PC\ or\ VS,sorbed,20\ \%}$ / $m_{PC\ or\ VS,fed,20\ \%}$ in the breakthrough tests (-) |
| $_{les,i}$ | C or VS desorption yield in a batch or breakthrough test, defined as $m_{PC\ or\ VS,desort}$ $n_{PC\ or\ VS,sorbed}$ (-) |
| | ffective porosity (-) |
| $_{esin}$ | esin operating capacity, defined as $m_{PC,sorbed,20\ \%}$ / $m_{PC,sorbed,saturation}$ (-) |

**References**:

[1] S. Dermeche, M. Nadour, C. Larroche, F. Moulti-Mati, P. Michaud, Olive mill wastes: Biochemical characterizations and valorization strategies, Process Biochem. 48 (2013) 1532-1552.

[2] L. Bertin, F. Ferri, A. Scoma, L. Marchetti, F. Fava, Recovery of high added value natural polyphenols from actual olive mill wastewater through solid phase extraction, Chem. Eng. J. 171 (2011) 1287-1293.

[3] N. Rahmanian, S.M. Jafari, C.M. Galanakis, Recovery and Removal of Phenolic Compounds from Olive Mill Wastewater, J. Am. Oil Chem. Soc. 91 (2014) 1-18.

[4] G. Pekin, S. Haskök, S. Sargın, Y. Gezgin, R. Eltem, E. İkizoğlu, N. Azbar, F.V. Sukan, Anaerobic digestion of Aegean olive mill effluents with and without pretreatment, J. Chem. Technol. Biotechnol. 85 (2010) 976-982.

[5] P. Paraskeva, E. Diamadopoulos, Technologies for Olive Mill Wastewater (OMW) Treatment: A Review, J. Chem. Technol. Biotechnol., 81 (2006) 1475-1485.

[6] P.S. Rodis, V.T. Karathanos, A. Mantzavinou, Partitioning of olive oil antioxidants between oil and water phases, J. Agric. Food Chem. 50 (2002) 596-601.

[7] D. Daassi, J. Lozano-Sanchez, I. Borras-Linares, L. Belbahri, S. Woodward, H. Zouari-Mechichi, T. Mechichi, M. Nasri, A. Segura-Carretero, Olive oil mill wastewaters: phenolic content characterization during degradation by Coriolopsis gallica, Chemosphere 113 (2014) 62-70.

[8] A. Cardinali, S. Pati, F. Minervini, I. D'Antuono, V. Linsalata, V. Lattanzio, Verbascoside, isoverbascoside, and their derivatives recovered from olive mill wastewater as possible food antioxidants, J. Agric. Food Chem. 60 (2012) 1822-1829.

[9] E. Aranda, I. Garcia-Romera, J.A. Ocampo, V. Carbone, A. Mari, A. Malorni, F. Sannino, A. De Martino, R. Capasso, Chemical characterization and effects on Lepidium sativum of the native and bioremediated components of dry olive mill residue, Chemosphere 69 (2007) 229-239.

[10] A. Fiorentino, A. Gentili, M. Isidori, P. Monaco, A. Nardelli, A. Parrella, F. Temussi, Environmental effects caused by olive mill wastewaters: toxicity comparison of low-molecular-weight phenol components, J. Agric. Food Chem. 51 (2003) 1005-1009.

[11] A. Rodriguez-Mateos, D. Vauzour, C.G. Krueger, D. Shanmuganayagam, J. Reed, L. Calani, P. Mena, D. Del Rio, A. Crozier, Bioavailability, bioactivity and impact on health of dietary flavonoids and related compounds: an update, Arch. Toxicol. 88 (2014) 1803-1853.

[12] D. Del Rio, A. Rodriguez-Mateos, J.P. Spencer, M. Tognolini, G. Borges, A. Crozier, Dietary (poly)phenolics in human health: structures, bioavailability, and evidence of protective effects against chronic diseases, Antioxid. Redox Signal 18 (2013) 1818-1892.

[13] P. Reboredo-Rodriguez, A. Varela-Lopez, T.Y. Forbes-Hernandez, M. Gasparrini, S. Afrin, D. Cianciosi, J. Zhang, P.P. Manna, S. Bompadre, J.L. Quiles, M. Battino, F. Giampieri, Phenolic Compounds Isolated from Olive Oil as Nutraceutical Tools for the Prevention and Management of Cancer and Cardiovascular Diseases, Int. J. Mol. Sci. 19 (2018) 2305.

[14] K.L. Tuck, P.J. Hayball, Major phenolic compounds in olive oil: metabolism and health effects, J. Nutr. Biochem. 13 (2002) 636-644.

[15] A. El-Abbassi, H. Kiai, A. Hafidi, Phenolic profile and antioxidant activities of olive mill wastewater, Food Chem. 132 (2012) 406-412.

[16] C. Fortes, J.A. García-Vilas, A.R. Quesada, M.Á. Medina, Evaluation of the anti-angiogenic potential of hydroxytyrosol and tyrosol, two bio-active phenolic compounds of extra virgin olive oil, in endothelial cell cultures, Food Chem. 134 (2012) 134-140.

[17] M. Araújo, F.B. Pimentel, R.C. Alves, M.B.P.P. Oliveira, Phenolic compounds from olive mill wastes: Health effects, analytical approach and application as food antioxidants, Trends Food Sci. Technol. 45 (2015) 200-211.

[18] N. Kalogerakis, M. Politi, S. Foteinis, E. Chatzisymeon, D. Mantzavinos, Recovery of antioxidants from olive mill wastewaters: a viable solution that promotes their overall sustainable management, J. Environ. Manage 128 (2013) 749-758.

[19] C.M. Galanakis, E. Tornberg, V. Gekas, Recovery and preservation of phenols from olive waste in ethanolic extracts, J. Chem. Technol. Biotechnol. 85 (2010) 1148-1155.

[20] D.P. Zagklis, A.I. Vavouraki, M.E. Kornaros, C.A. Paraskeva, Purification of olive mill wastewater phenols through membrane filtration and resin adsorption/desorption, J. Hazard. Mater. 285 (2015) 69-76.

[21] C. Conidi, R. Mazzei, A. Cassano, L. Giorno, Integrated membrane system for the production of phytotherapics from olive mill wastewaters, J. Membr. Sci. 454 (2014) 322-329.

[22] L. Bertin, D. Frascari, H. Domínguez, E. Falqué, F.A. Riera Rodriguez, S. Alvarez Blanco, Conventional purification and isolation, in: C.M. Galanakis (Ed.) Food Waste Recovery: Processing Technologies and Techniques, Elsevier - Academic Press, London, 2015, pp. 149-172.

[23] M.L. Soto, A. Moure, H. Domínguez, J.C. Parajó, Recovery, concentration and purification of phenolic compounds by adsorption: A review, J. Food Eng. 105 (2011) 1-27.

[24] M. El Idrissi, A.E. Molina Bacca, D. Frascari, P.F.X. Corvini, P. Shahgaldian, Cyclodextrin-based polymeric materials for the specific recovery of polyphenolic compounds through supramolecular host–guest interactions, J. Incl. Phenom. Macrocycl. Chem. 88 (2017) 35-42.

[25] D. Frascari, A.E.M. Bacca, F. Zama, L. Bertin, F. Fava, D. Pinelli, Olive mill wastewater valorisation through phenolic compounds adsorption in a continuous flow column, Chem. Eng. J. 283 (2016) 293-303.

[26] D. Frascari, G. Zanaroli, M.A. Motaleb, G. Annen, K. Belguith, S. Borin, R. Choukr-Allah, C. Gibert, A. Jaouani, N. Kalogerakis, F. Karajeh, P.A. Ker Rault, R. Khadra, S. Kyriacou, W.T. Li, B. Molle, M. Mulder, E. Oertle, C.V. Ortega, Integrated technological and management solutions for wastewater treatment and efficient agricultural reuse in Egypt, Morocco, and Tunisia, Integr. Environ. Assess. Manag. 14 (2018) 447-462.

[27] A. El-Abbassi, H. Kiai, J. Raiti, A. Hafidi, Cloud point extraction of phenolic compounds from pretreated olive mill wastewater, J. Environ. Chem. Eng. 2 (2014) 1480-1486.

[28] M. Caetano, C. Valderrama, A. Farran, J.L. Cortina, Phenol removal from aqueous solution by adsorption and ion exchange mechanisms onto polymeric resins, J. Colloid Interface Sci. 338 (2009) 402-409.

[29] L. Zhu, Y. Deng, J. Zhang, J. Chen, Adsorption of phenol from water by N-butylimidazolium functionalized strongly basic anion exchange resin, J. Colloid Interface Sci. 364 (2011) 462-468.

[30] Y. Ku, K.-C. Lee, Removal of phenols from aqueous solution by XAD-4 resin, J. Hazard. Mater. 80 (2000) 59-68.

[31] M. Carmona, A.D. Lucas, J.L. Valverde, B. Velasco, J.F. Rodríguez, Combined adsorption and ion exchange equilibrium of phenol on Amberlite IRA-420, Chem. Eng. J. 117 (2006) 155-160.

[32] D. Pinelli, A.E. Molina Bacca, A. Kaushik, S. Basu, M. Nocentini, L. Bertin, D. Frascari, Batch and Continuous Flow Adsorption of Phenolic Compounds from Olive Mill Wastewater: A Comparison between Nonionic and Ion Exchange Resins, Int. J. Chem. Eng. 2016 (2016) 13.

[33] E. Bazrafshan, P. Amirian, A.H. Mahvi, A. Ansari-Moghaddam, Application Of Adsorption Process For Phenolic Compounds Removal From Aqueous Environments: A Systematic Review, Global Nest J. 18 (2016) 146-163.

[34] J. Kammerer, D.R. Kammerer, R. Carle, Impact of saccharides and amino acids on the interaction of apple polyphenols with ion exchange and adsorbent resins, J. Food Eng. 98 (2010) 230-239.

[35] J. Kammerer, R. Carle, D.R. Kammerer, Adsorption and ion exchange: basic principles and their application in food processing, J. Agric. Food Chem. 59 (2011) 22-42.

[36] C. Datta, A. Dutta, D. Dutta, S. Chaudhuri, Adsorption of polyphenols from ginger rhizomes on an anion exchange resin Amberlite IR-400 – Study on effect of pH and temperature, Procedia Food Science 1 (2011) 893-899.

[37] Z.P. Gao, Z.F. Yu, T.L. Yue, S.Y. Quek, Adsorption isotherm, thermodynamics and kinetics studies of polyphenols separation from kiwifruit juice using adsorbent resin, J. Food Eng. 116 (2013) 195-201.

[38] X. Jiao, B. Li, X. Zhang, Q. Zhang, N. Gao, X. Meng, Optimation of Enrichment and Purification of Polyphenols from Blueberries (Vaccinium spp) by Macroporous Resins XAD-7HP, Emir. J. Food Agric. 29 (2018) 581-588.

[39] X. Jiang, W. Yang, C. Zhou, K. Lu, C. Lin, Separation and Purification of Polyphenols from Pericarpium Granati Using Macroporous Resins and Evaluation of its Anti-Streptococcus mutans Activity in vitro, Biotechnology(Faisalabad) 15 (2016) 86-95.

[40] A. Agalias, P. Magiatis, A.L. Skaltsounis, E. Mikros, A. Tsarbopoulos, E. Gikas, I. Spanos, T. Manios, A new process for the management of olive oil mill waste water and recovery of natural antioxidants, J. Agric. Food Chem. 55 (2007) 2671-2676.

[41] M. Ziati, F. Khemmari, O. Cherifi, F.Y. Didouche, Removal of polyphenols from olive mill wastewater by adsorption on activated carbon prepared from peach stones, Rev. Roum. Chim 62 (2017), 865-874.

[42] P.J.E. Harlick, F.H. Tezel, An experimental adsorbent screening study for CO2 removal from N2, Microporous Mesoporous Mater. 76 (2004) 71-79.

[43] ASTM International, Standard Practice for Selection of Sorbents, Sampling, and Thermal Desorption Analysis Procedures for Volatile Organic Compounds in Air N. D 6196 – 03, West Conshohocken, PA (2003) .

[44] Y.W. Chiang, R.M. Santos, K. Ghyselbrecht, V. Cappuyns, J.A. Martens, R. Swennen, T. Van Gerven, B. Meesschaert, Strategic selection of an optimal sorbent mixture for in-situ remediation of heavy metal contaminated sediments: Framework and case study, J. Environ. Manage. 105 (2012) 1-11.

[45] O. Folin, V. Ciocalteu, On tyrosine and tryptophane determinations in protein, J. Biol. Chem. 73 (1927) 627-650.

[46] L. Bresciani, L. Calani, M. Cossu, P. Mena, M. Sayegh, S. Ray, D. Del Rio, (Poly)phenolic characterization of three food supplements containing 36 different fruits, vegetables and berries, PharmaNutrition 3 (2015) 11-19.

[47] I. Leouifoudi, H. Harnafi, A. Zyad, Olive Mill Waste Extracts: Polyphenols Content, Antioxidant, and Antimicrobial Activities, Adv. Pharmacol. Sci. 2015 (2015) 714138.

[48] M.M. Bradford, A rapid and sensitive method for the quantitation of microgram quantities of protein utilizing the principle of protein-dye binding, Anal. Biochem. 72 (1976) 248-254.

[49] G.L. Miller, Use of Dinitrosalicylic Acid Reagent for Determination of Reducing Sugar, Anal. Chem. 31 (1959) 426-428.

[50] Y.S. Ho, G. McKay, Pseudo-second order model for sorption processes, Process Biochem. 34 (1999) 451-465.

[51] K.Y. Foo, B.H. Hameed, Insights into the modeling of adsorption isotherm systems, Chem. Eng. J. 156 (2010) 2-10.

[52] M. Abdelkreem, Adsorption of Phenol from Industrial Wastewater Using Olive Mill Waste, APCBEE Procedia 5 (2013) 349-357.

[53] D. Frascari, G. Zanaroli, G. Bucchi, A. Rosato, N. Tavanaie, S. Fraraccio, D. Pinelli, F. Fava, Trichloroethylene aerobic cometabolism by suspended and immobilized butane-growing microbial consortia: a kinetic study, Bioresour. Technol. 144 (2013) 529-538.

[54] L.H. Smith, P.K. Kitanidis, P.L. McCarty, Numerical modeling and uncertainties in rate coefficients for methane utilization and TCE cometabolism by a methane-oxidizing mixed culture, Biotechnol. Bioeng. 53 (1997) 320-331.

[55] O. Levenspiel, Chemical Reaction Engineering., John Wiley & Sons, New York, 1999.

[56] A. Scoma, C. Pintucci, L. Bertin, P. Carlozzi, F. Fava, Increasing the large scale feasibility of a solid phase extraction procedure for the recovery of natural antioxidants from olive mill wastewaters, Chem. Eng. J. 198-199 (2012) 103-109.

[57] Y. Achmon, A. Fishman, The antioxidant hydroxytyrosol: biotechnological production challenges and opportunities, Appl. Microbiol. Biotechnol. 99 (2015) 1119-1130.

[58] R. Rossi, S. Ratti, G. Pastorelli, F. Maghin, G. Martemucci, D. Casamassima, A.G. D'Alessandro, C. Corino, Effect of dietary plant extract on meat quality and sensory parameters of meat from Equidae, J. Sci. Food Agric. 97 (2017) 4690-4696.

[59] DOW (Trademark of The Dow Chemical Company), Tech Fact - Ion Exchange Resins Selectivity, 2016.

[60] J. Perez-Jimenez, V. Neveu, F. Vos, A. Scalbert, Identification of the 100 richest dietary sources of polyphenols: an application of the Phenol-Explorer database, Eur. J. Clin. Nutr. 64 Suppl 3 (2010) S112-120.

[61] D. Huang, B. Ou, R.L. Prior, The chemistry behind antioxidant capacity assays, J. Agric. Food Chem. 53 (2005) 1841-1856.

[62] L.M. Magalhaes, M.A. Segundo, S. Reis, J.L. Lima, A.O. Rangel, Automatic method for the determination of Folin-Ciocalteu reducing capacity in food products, J. Agric. Food Chem. 54 (2006) 5241-5246.

[63] L.M. Magalhaes, M.A. Segundo, S. Reis, J.L. Lima, Methodological aspects about in vitro evaluation of antioxidant properties, Anal. Chim. Acta 613 (2008) 1-19.

[64] B. Aliakbarian, A.A. Casazza, P. Perego, Kinetic and Isotherm Modelling of the Adsorption of Phenolic Compounds from Olive Mill Wastewater onto Activated Carbon, Food Technol. Biotechnol. 53 (2015) 207-214.

[65] F. Ferri, L. Bertin, A. Scoma, L. Marchetti, F. Fava, Recovery of low molecular weight phenols through solid-phase extraction, Chem. Eng. J. 166 (2011) 994-1001.

[66] M. Navarro, F.J. Morales, Effect of hydroxytyrosol and olive leaf extract on 1,2-dicarbonyl compounds, hydroxymethylfurfural and advanced glycation endproducts in a biscuit model, Food Chem. 217 (2017) 602-609.

[67] S. Abu-Lafi, M.S. Al-Natsheh, R. Yaghmoor, F. Al-Rimawi, Enrichment of Phenolic Compounds from Olive Mill Wastewater and In Vitro Evaluation of Their Antimicrobial Activities, Evid. Based Complement Alternat. Med. 2017 (2017) 3706915.

[68] L. Martinez, G. Ros, G. Nieto, Hydroxytyrosol: Health Benefits and Use as Functional Ingredient in Meat, Medicines (Basel) 5 (2018).

[69] H. Tavakoli, O. Hosseini, S.M. Jafari, I. Katouzian, Evaluation of Physicochemical and Antioxidant Properties of Yogurt Enriched by Olive Leaf Phenolics within Nanoliposomes, J Agric Food Chem. 66 (2018) 9231-9240.

[70] I. Aissa, N. Kharrat, F. Aloui, M. Sellami, M. Bouaziz, Y. Gargouri, Valorization of antioxidants extracted from olive mill wastewater, Biotechnol. Appl. Biochem. 64 (2017) 579-589.

**Table 1**

Average characteristics of the raw and microfiltered OMW (average values ± 95% confidence intervals).

| Parameter | Raw OMW | Microfiltered OMW |
|---|---|---|
| Total phenolic compounds ($g_{AG\,eq.}$/L; HPLC method) | 1.41 ± 0.08 | 1.28 ± 0.07 |
| Total phenolic compounds ($g_{AG\,eq.}$/L; Folin method) | 4.4 ± 0.5 | 4.0 ± 0.3 |
| Total solids (g/L) | 41 ± 1 | 37 ± 1 |
| Volatile solids (g/L) | 25 ± 0.5 | 22 ± 0.5 |
| Suspended solids (g/L) | 3.5 ± 0.1 | 0.005 ± 0.001 |
| Dissolved solids (g/L) | 38 ± 1 | 38 ± 1 |
| COD (g/L) | 70 ± 5 | 65 ± 4 |
| Reducing sugars (g/L) | 3.5 ± 0.3 | 5.1 ± 0.1 |
| Proteins ($g_{BSA}$/L) | 0.15 ± 0.02 | 0.21 ± 0.02 |
| pH | 4.24 ± 0.08 | 4.21 ± 0.09 |
| Antioxidant capacity ($mM_{AAeq}$) | 15 ± 1 | 13 ± 1 |

**Table 2**

Identified PCs in the raw OMW and in the desorbed products obtained with resins XAD16N and IRA958 OH, with spectrometric characteristics.

| Compound | Retention time | Mass / charge ratio (m/z) | MS2 Fragmentation[a] | Raw OMW[b] | XAD16N desorbed product[b] | IRA958 OH desorbed product[b] |
|---|---|---|---|---|---|---|
| ***Phenolic acids*** | | | | | | |
| Gallic acid | 2.22 | 169 | 125 | n | n | y |
| 3,4-Dihydroxyphenylacetic acid | 3.23 | 167 | 123 | y | y | y |
| 3,4-Dihydroxybenzoic acid | 3.68 | 153 | 123, 109 | y | y | y |
| Dihydroxybenzoic acid [c] | 3.89 | 153 | 123, 121, 109 | y | y | n |
| Dihydroxybenzoic acid [c] | 4.49 | 153 | 123, 125, 109 | y | y | y |
| Homovanillic acid | 4.60 | 181 | 137 | y | y | y |
| Hydroxybenzoic acid | 4.60 | 137 | 93 | y | y | y |
| p-Coumaric acid | 4.82 | 163 | 119 | n | y | y |
| Caffeic acid | 5.14 | 179 | 135 | y | y | y |
| Vanillic acid | 5.25 | 167 | 152, 123 | n | y | n |
| o-Coumaric acid [c] | 5.82 | 163 | 119 | n | n | y |
| cis-Ferulic acid | 5.99 | 193 | 149, 178, 134 | n | y | n |
| Trimethoxybenzoic acid | 6.15 | 211 | 167 | y | y | n |
| Syringic acid | 6.25 | 197 | na[d] | y | y | n |
| trans-Ferulic acid | 6.49 | 193 | 149, 178, 134 | n | y | n |
| ***Phenylethanoids and Secoiridoids*** | | | | | | |
| Hydroxytyrosol hexoside | 3.38 | 315 | 153 | n | y | y |
| Hydroxytyrosol | 3.45 | 153 | 123 | y | y | y |
| Tyrosol | 3.80 | 137 | 109 | n | n | y |
| Oleoside | 4.47 | 389 | 345 | n | y | n |
| Hydroxyelanolic acid | 4.54 | 257 | 239 | y | n | n |
| Hydroxyverbascoside | 5.32 | 639 | 621, 529, 459 | y | y | y |
| Elanolic acid | 5.32 | 241 | 165, 183, 197, 223 | y | y | n |
| Hydroxyverbascoside | 5.69 | 639 | 621, 529 | n | n | y |
| Elanolic acid | 5.86 | 241 | 165, 197, 213 | y | y | n |
| Verbascoside [c] | 5.96 | 623 | 461 | y | y | y |
| Verbascoside [c] | 6.36 | 623 | 461 | n | n | y |
| Hydroxytyrosol acetate [c] | 6.57 | 195 | na[d] | n | y | n |
| Hydroxytyrosol acetate [c] | 6.86 | 195 | na[d] | n | n | y |
| Elanolic acid | 6.88 | 241 | 209, 165, 139 | n | y | n |
| Oleuropein [c] | 7.00 | 539 | 377, 307, 275 | y | y | y |
| Oleuropein [c] | 7.31 | 539 | 377, 307, 275 | y | y | y |
| Oleuropein aglycone | 8.25 | 377 | 241 | y | y | y |
| ***Flavonoids*** | | | | | | |
| Rutin | 6.08 | 609 | 301, 300 | n | y | n |
| Apigenin | 7.88 | 269 | 225, 209, 251 | n | y | n |
| ***Lignans*** | | | | | | |
| Pinoresinol | 8.92 | 357 | 311 | n | y | n |

[a] MS2 fragmentation indicates the fragmentation of the parent ion. [b] y, detected; n, not detected.
[c] Tentative identification. The same name reported for some compounds indicates different isomers, characterized by different retention time and which probably differ for the position of the substituent groups. [d] na: not available. The parent ion has not been fragmented.

**Table 3**

Simulations of the isotherms conducted with the 5 tested resins: best-fitting parameters ± 95% confidence intervals and $R^2$ values obtained with both the Langmuir and Freundlich models for PCs and only with the Freundlich model for COD; estimate of the sorbed PC and COD concentrations in equilibrium with the corresponding concentrations in the microfiltered OMW; estimate of the purity of the sorbed product.

| Resin | PC: Langmuir parameters | | | PC: Freundlich parameters | | | Best fitting model for PCs | F test | | COD: Freundlich parameters | | | Sorbed concentrations in equilibrium with OMW | | Sorbed product purity | |
|---|---|---|---|---|---|---|---|---|---|---|---|---|---|---|---|---|
| | $C_{S,PC}^{\infty}$ (mg$_{PC}$/ g$_{dry\ resin}$) | $K_{eq,PC}$ (L/g$_{PC}$) | $R^2$ | $K_{F,PC}$ (L/g$_{dry\ resin}$) | $n_{PC}$ (-) | $R^2$ | | $p^a$ | Statistical difference | $K_{F,COD}$ (L/g$_{dry\ resin}$) | $n_{COD}$ (-) | $R^2$ | $C_{s,PC,eqOMW}^b$ (mg$_{PC}$/ g$_{dry\ resin}$) | $C_{s,COD,eqOMW}^b$ (g$_{O2}$/ g$_{dry\ resin}$) | PC/COD (g$_{PC}$ /g$_{COD}$) | PC/VS (g$_{PC}$ /g$_{VS}$) |
| XAD761 | 104±18 | (1.1±0.3)·10$^{-3}$ | 0.988 | 0.38±0.02 | 1.38±0.02 | 0.986 | Langmuir | 36% | No | (2.9±2.3)·10$^{-4}$ | 0.52±0.13 | 0.933 | 60±13 | 0.9±1.3 | 0.07±0.06 | 0.20±0.16 |
| XAD16N | 111±8 | (2.1±0.3)·10$^{-3}$ | 0.996 | 1.14±0.33 | 1.62±0.14 | 0.990 | Langmuir | 4.5% | Yes | (3.5±2.9)·10$^{-4}$ | 0.51±0.12 | 0.940 | 81±7 | 1.2±1.7 | 0.07±0.05 | 0.19±0.16 |
| FPX66 | 82±5 | (3.3±0.5)·10$^{-3}$ | 0.995 | 1.48±0.52 | 1.79±0.21 | 0.978 | Langmuir | 0.4% | Yes | (2.0±1.9)·10$^{-4}$ | 0.45±0.07 | 0.976 | 67±5 | 2.1±1.0 | 0.03±0.02 | 0.09±0.05 |
| Optipore SD-2 | 41±5 | (1.2±0.5)·10$^{-2}$ | 0.950 | 3.54±0.96 | 2.77±0.37 | 0.981 | Freundlich | 3.6% | Yes | (1.4±0.8)·10$^{-3}$ | 0.58±0.07 | 0.980 | 47±13 | 1.8±1.1 | 0.03±0.02 | 0.07±0.05 |
| IRA958 OH | 725±140 | (4.9±1.0)·10$^{-5}$ | 0.846 | (2.1±0.6)·10$^{-3}$ | 0.71±0.26 | 0.902 | Freundlich | 19% | No | (4.6±1.6)·10$^{-5}$ | 0.41±0.19 | 0.908 | 48±15 | 1.2±0.4 | 0.04±0.02 | 0.12±0.05 |

[a] Probability that the best fits obtained with the Langmuir and Freundlich models are not statistically different. Significance level = 5%.

[b] Sorbed PC and COD concentrations in equilibrium with the corresponding concentrations in the microfiltered OMW.

**Table 4**

Adsorption and desorption performances relative to the breakthrough tests conducted with resins XAD16N and IRA958 OH in the 1-m packed column (average values ± 95% confidence intervals).

| Parameter | XAD16N | IRA958 OH |
|---|---|---|
| Resin effective porosity ($\varepsilon$, -) | 0.70±0.01 | 0.49±0.02 |
| HRT in the resin (h) | 0.30±0.01 | 0.33±0.02 |
| Superficial velocity (m/h) | 2.30±0.02 | 1.47±0.02 |
| Bed volumes / h (BV/h, 1/h) | 2.30±0.02 | 1.47±0.02 |
| PC adsorption yield at 20% PC breakpoint ($Y_{ads,PC}$, -) | 0.93±0.08 | 0.96±0.08 |
| VS adsorption yield at 20% PC breakpoint ($Y_{ads,VS}$, -) | 0.26±0.06 | 0.69±0.15 |
| Resin selectivity for PCs at 20% PC breakpoint ($Y_{ads,PC}$ / $Y_{ads,VS}$) | 3.6±0.8 | 1.4±0.3 |
| PC operating capacity at 20% PC breakpoint ($\eta_{PC}$, -) | 0.30±0.02 | 0.10±0.01 |
| Sorbed product purity at 20% PC breakpoint ($g_{PC}/g_{VS}$) | 0.14±0.03 | 0.03±0.01 |
| Sorbed product purity at end of test ($g_{PC}/g_{VS}$) | 0.39±0.10 | 0.22±0.06 |
| PC desorption yield ($Y_{des,PC}$, -) | 0.87±0.05 | 0.95±0.05 |
| VS desorption yield ($Y_{des,VS}$, -) | 0.99±0.04 | 0.99±0.04 |

**Table 5**

Relative composition of the desorbed products obtained from resins XAD16N and IRA958 OH and of the microfiltered OMW fed to the adsorption process (average values ± 95% confidence intervals).

| Parameter | Microfiltered OMW | XAD16N desorbed product | IRA958 OH desorbed product |
|---|---|---|---|
| Product purity ($g_{PC}/g_{VS}$; HPLC method for PCs) | 0.060±0.004 | 0.210±0.013 | 0.190±0.012 |
| Product purity ($g_{PC}/g_{VS}$; Folin method for PCs) | 0.18±0.02 | 0.34±0.03 | 0.41±0.04 |
| Specific antioxidant capacity ($g_{AAeq}/g_{PC}$)[a] | 5.3±0.4 | 4.9±0.4 | 4.6±0.3 |
| Reducing sugars ($g_{sugars}/g_{VS}$) | 0.23±0.01 | 0.30±0.02 | 0.56±0.03 |
| Protein content ($g_{BSA}/g_{VS}$) | 0.010±0.001 | 0.040±0.005 | 0.090±0.010 |
| Volatile solid content ($g_{VS}/g_{TS}$) | 0.59±0.02 | 0.99±0.04 | 0.92±0.03 |

[a] The (ascorbic acid)/(PC) ratio refers to the total PC content quantified by HPLC.

**Fig. 1.** Flow sheet and picture of the adsorption / desorption plant. 1, tank for raw OMW or desorption solvent; 2, centrifugal pump; 3, sampling point for raw OMW or desorption solvent;

4, microfiltration unit; 5, sampling point for microfiltered OMW; 6, first column; 7, second column;

8, sampling point for effluent of the adsorption / desorption process; 9, tank for dephenolized OMW or PC-rich desorption solvent. The microfiltration unit – not shown in the picture - was bypassed during the desorption process. Of the four columns visible in the picture, two were dedicated to the breakthrough tests conducted with 1 of the 2 best-performing resins identified by means of the isotherm batch tests, whereas the other 2 were dedicated to the tests conducted with the other best-performing resin.
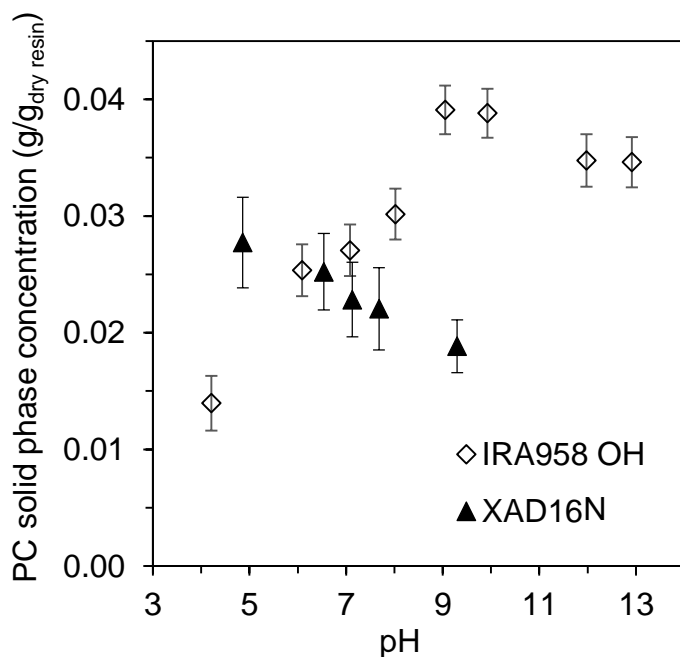


**Fig. 2.** Resins IRA958 OH and XAD16N: PC solid phase concentration versus pH in single-point batch tests conducted at 10 $g_{dry\ resin}/L_{OMW}$.
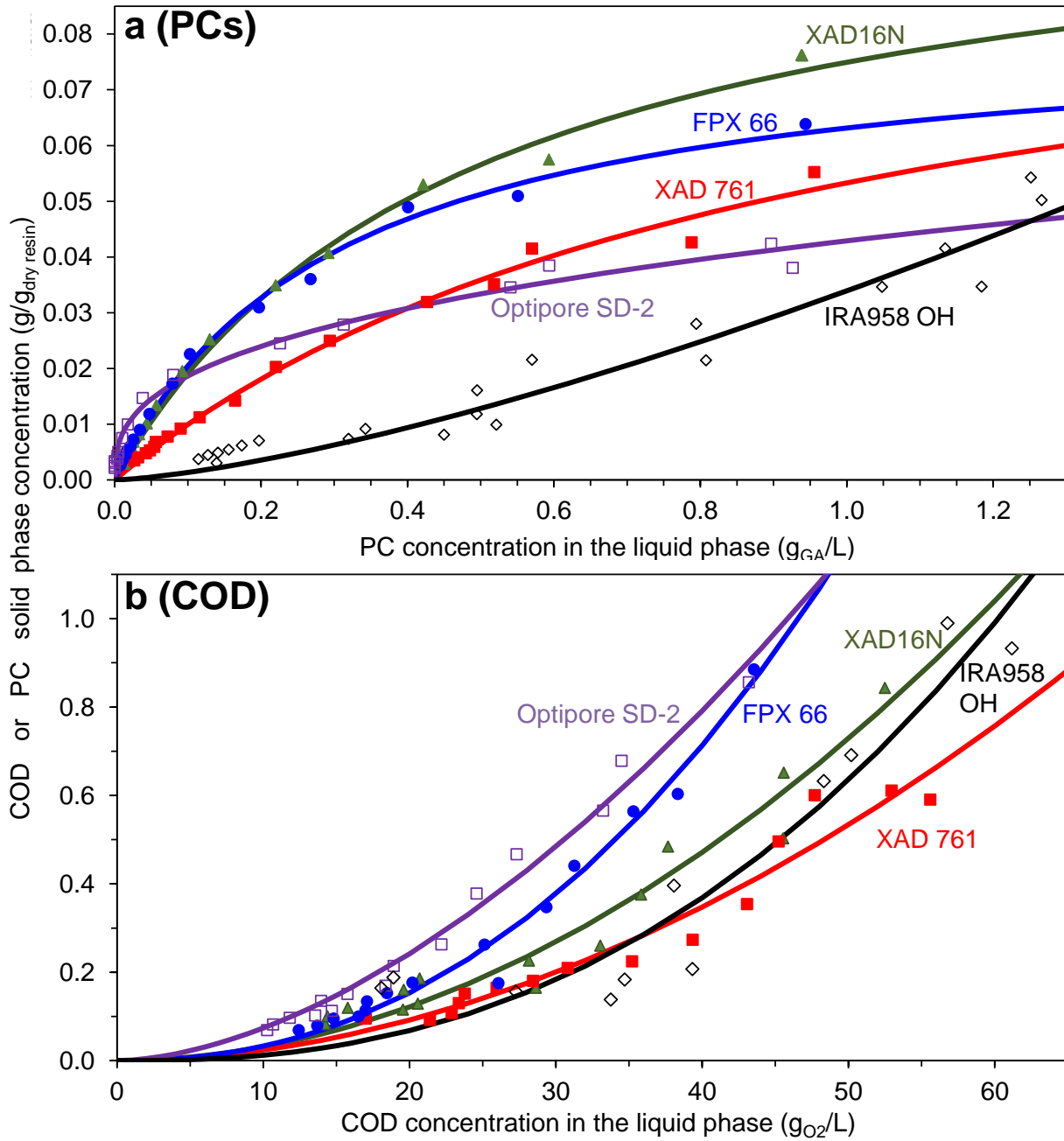
**Fig. 3.** Batch isotherms conducted with the 5 tested resins: PC (a) and COD (b) solid phase versus liquid phase concentrations and best-fitting interpolations obtained with the Langmuir (Eq. 2) or Freundlich (Eq. 3) model. For the PC isotherms, the best-fitting model is specified in Table 3, whereas all the COD isotherms were interpolated with the Freundlich model.
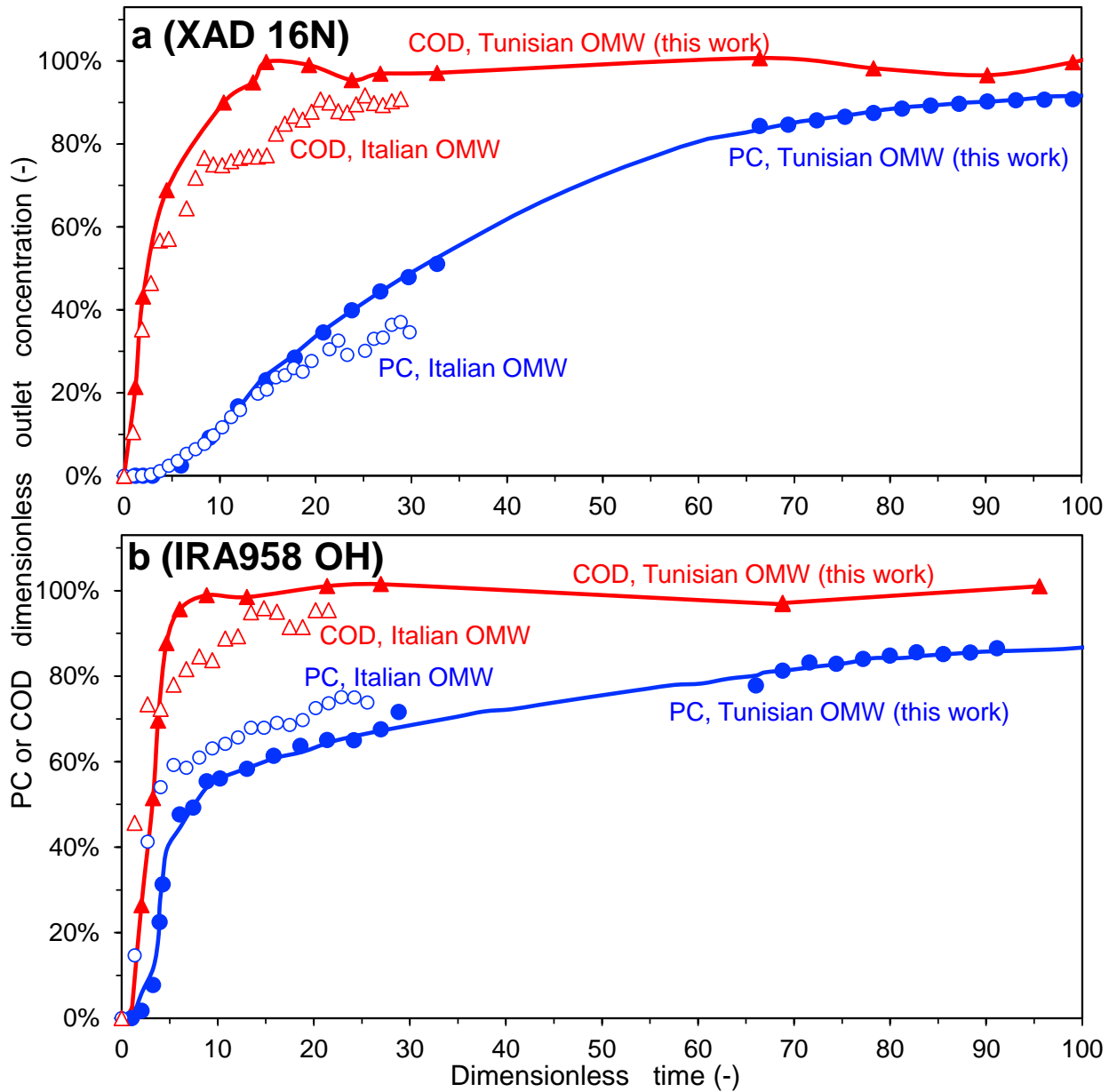
**Fig. 4.** Normalized PC and COD concentrations at the column outlet versus dimensionless time (actual time / HRT) during continuous-flow breakthrough tests conducted with resins XAD16N (a) and IRA958 OH (b). Full symbols refer to the tests conducted in the framework of this work with Tunisian OMW and described in detail in section 3.5 and Table 4. In these tests, the PC and COD experimental points are connected by interpolating lines drawn to make the figure more readable. For comparison purposes, empty symbols refer to the PC and COD time plots obtained with the same HRT in previous studies conducted with an Italian OMW, significantly different than the Tunisian one object of this work.

# Valorisation of olive mill wastewater by phenolic compounds adsorption: development and application of a procedure for adsorbent selection

Dario Frascari, Giorgia Rubertelli, Fatma Arous, Alessandro Ragini, Letizia Bresciani, Antonio Arzu, Davide Pinelli

## SUPPLEMENTARY MATERIAL

**Table S1**

Technical characteristics of the tested resins.

| Resin | Adsorption mechanism | Matrix | Surface Area $(m^2/g)$ | Pore size $(A)$ | Harmonic mean particle size (mm) | Approximate industrial cost (€/L) |
|---|---|---|---|---|---|---|
| XAD761 | Neutral adsorption | Crosslinked phenol-formaldehyde polycondensate | 200 | 600 | 0.56 – 0.76 | 28 |
| XAD16N | Neutral adsorption | Macroporous styrene-divinylbenzene copolymer | 800 | 150 | 0.56 – 0.71 | 31 |
| FPX66 | Neutral adsorption | | 700 | 150 | 0.60 – 0.75 | 26 |
| OPTIPORE SD-2 | Neutral adsorption + minor ion exchange component | | 800 | 50 | [a] | 18 |
| IRA958 Cl | Strong ion exchange | Crosslinked acrylic polymer with quaternary ammonium group | 400 | [a] | 0.63-0.85 | 8 |

[a] Data not available

**Table S2**
Procedure for the evaluation of the performance indicators obtained from the breakthrough tests.

---

**1) PC and VS adsorption yield ($Y_{ads,i}$)**

$Y_{ads,i}$, was evaluated at a 0.20 PC breakpoint as $m_{i,sorbed,20\%} / m_{i,fed,20\%}$, where $m_{i,sorbed,20\%}$ indicates the PC or VS mass adsorbed until the attainment of a 20% outlet normalized PC concentration, and $m_{i,fed,20\%}$ indicates the corresponding PC or COD mass fed to the adsorption column. $m_{i,sorbed,20\%}$ was estimated as:

$$m_{i,sorbed,20\%} = m_{i,fed,20\%} - m_{i,out,20\%} \tag{S1}$$

where $m_{i,out,20\%}$ is the mass lost in the outlet up to the 20% breakpoint. Eq. (S1) does not take into consideration the liquid phase PC content at the 20% breakthrough point, which is generally negligible. $m_{i,out,20\%}$ was calculated by numerical integration of the experimental breakthrough curve up to the selected 20% PC breakpoint:

$$m_{i,out,20\%} = Q \cdot \int_0^{t_{20\%}} C_{L,i,OUT} \cdot dt \tag{S2}$$

where $Q$ indicates the OMW flow rate fed to the column.

---

**2) Resin operating capacity ($\eta_{resin}$)**

$\eta_{resin}$ was evaluated at a 0.20 PC breakpoint as $m_{PC,sorbed,20\%} / m_{PC,sorbed,saturation}$. $m_{PC,sorbed,saturation}$ indicates the PC mass theoretically adsorbed by the resin upon saturation of the sorption capacity. Since all the breakthrough tests conducted in this work were continued until the attainment of an outlet PC concentration close to the inlet PC concentration (condition of resin saturation), $m_{PC,sorbed,saturation}$ was calculated by numerical integration of the experimental breakthrough curve until the last experimental point:

$$m_{PC,sorbed,saturation} = Q \cdot \int_0^{t_{final}} \left( C_{L,PC,IN} - C_{L,PC,OUT} \right) \cdot dt \tag{S3}$$

where $Q$ indicates the OMW flow rate fed to the column.

---

**3) PC and VS desorption yield ($Y_{des,i}$)**

$Y_{des,i}$, was evaluated as $m_{i, desorbed} / m_{i,sorbed}$. $m_{i, desorbed}$ was calculated by numerical integration of the experimental curve of PC or VS concentration obtained at the column outlet during the desorption procedure:

$$m_{i, desorbed} = Q_{des} \cdot \int_0^{t_{final}} C_{L,i,OUT} \cdot dt \tag{S4}$$

where $Q_{des}$ indicates the desorption solvent flow rate fed to the column.

**Table S3**
Schematic representation of the proposed procedure for the identification of the most suitable resin(s), desorption solvent(s) and operational conditions for the recovery of PCs from liquid agro-industrial wastes.

| Step | Type of test | Short test description | Output: performance parameters (PP) and operational conditions (OC) |
|---|---|---|---|
| 1 | Single point batch tests | Batch tests aimed at identifying the best pH for the tested resins | OC: Optimal pH for the tested resins |
| 2 | Batch adsorption isotherms | Batch tests; 10-15 resin/liquid ratios for each tested resin | PP: PC sorbed concentration in equilibrium with the PC average concentration in the liquid waste<br>PP: Purity of the sorbed product ($g_{PC}/g_{VS}$) |
| 3 | Batch desorption isotherms | Preliminary tests aimed at identifying a suitable desorption solvent and desorption conditions | OC: optimal desorption solvent(s)<br>OC: optimal pH for the desorption process |
| 4 | Breakthrough adsorption tests | Continuous flow adsorption tests | PP: PC and VS adsorption yield and resin selectivity for PCs ($Y_{ads,PC}/Y_{ads,VS}$)<br>PP: Resin PC operating capacity |
| 5 | Breakthrough desorption tests | Continuous flow desorption tests | PP: PC and VS desorption yield<br>PP: Specific antioxidant capacity of the desorbed product;<br>PP: Purity of the desorbed product ($g_{PC}/g_{VS}$)<br>PP: Presence in the desorbed product of high-value specific compounds |
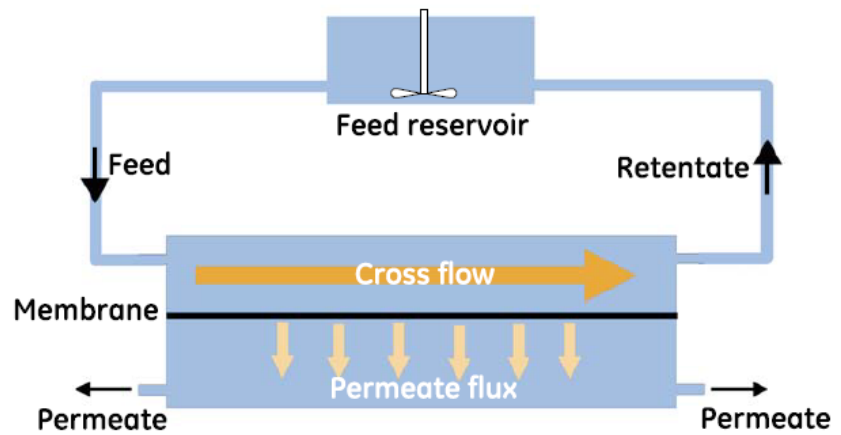
**Fig. S1.** Picture and flow sheet of the OMW microfiltration plant. The technique implemented in this filtration unit is cross flow filtration, also known as tangential flow filtration, in which the feed suspension passes tangentially along the surface of the filter. A pressure difference drives through the filter the components that are smaller than the pores (average pore-size = 0.2 µm). The filter contains a network of grooves, all connected to the same outlet line. Components larger than the filter pores are retained and pass along the membrane surface, flowing back to the feed reservoir. The filtration process continues until the pressure required to filter the wastewater exceeds the operational pressure pump threshold, or when the feed wastewater volume is equal to the dead volume of the system (about 4 L).
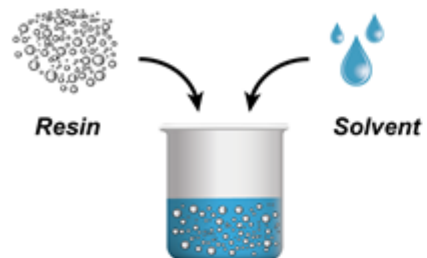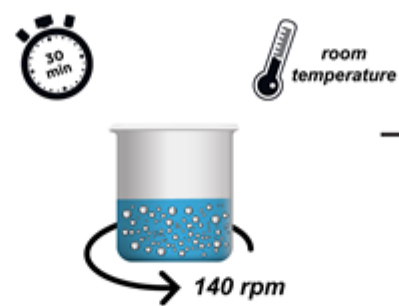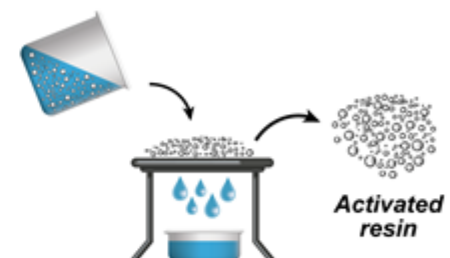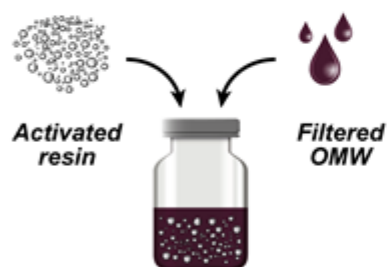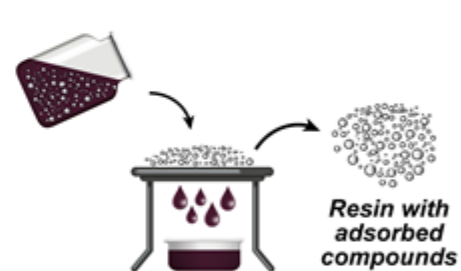
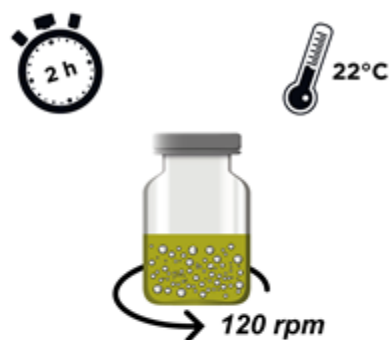**Fig. S2.** Schematic representation of the procedure for resin activation and for the operation of the adsorption isotherm tests
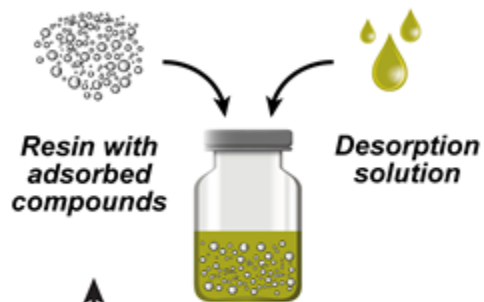
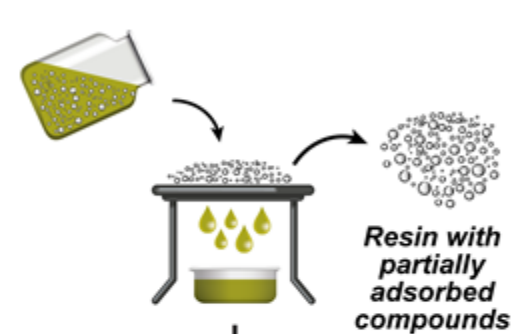**Fig. S3.** Schematic representation of the procedure for the operation of the desorption isotherm tests
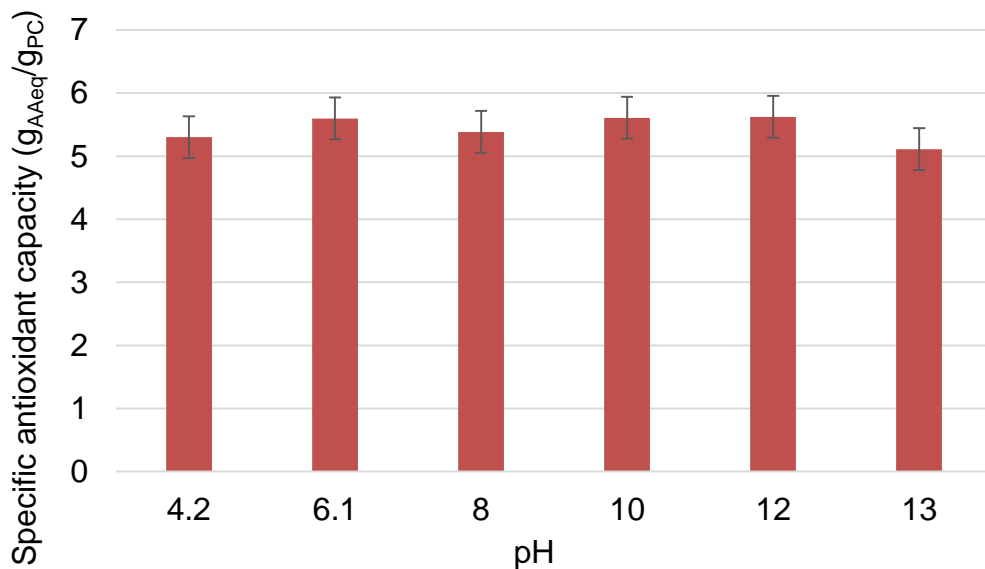
**Fig. S4.** Specific antioxidant activity of the microfiltered OMW at different pH values.
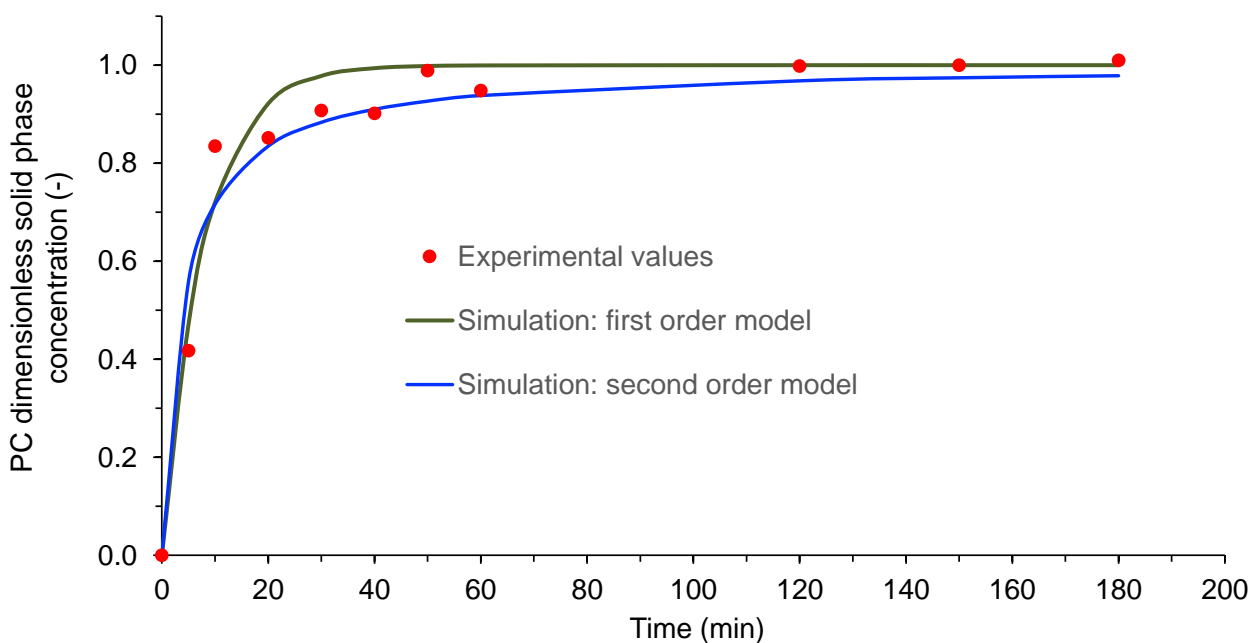


**Fig. S5.** Dimensionless sorbed-phase concentration ($C^*_{S,PC,t} = C_{S,PC,t} / C_{S,PC,eq}$, where $C_{S,PC,eq}$ indicates the average sorbed-phase concentration during the last 30 minutes of each test) versus time in the kinetic adsorption test conducted with resin XAD16N: experimental data and best-fitting interpolations obtained with the first-order or Lagergren model ($dC^*_{S,PC,t}/dt = k_1 \cdot (C^*_{S,PC,eq} - C^*_{S,PC,t})$) and the pseudo-second-order model ($dC^*_{S,PC,t}/dt = k_2 \cdot (C^*_{S,PC,eq} - C^*_{S,PC,t})^2$) [50].
Best fitting values of the model parameters:
- first order model: $k_1$ = 0.127  1/min
- second order model: $k_2$ = 0.00615 $g_{dry\ resin}$ / ($mg_{PC}$ min).